

37. PALEOCENE TO MIDDLE EOCENE CALCAREOUS NANNOFOSSILS OF ODP SITES 689 AND 690, MAUD RISE, WEDDELL SEA¹

James J. Pospichal² and Sherwood W. Wise, Jr.²

ABSTRACT

Cores from Sites 689 and 690 of Ocean Drilling Program Leg 113 provide the most continuous Paleocene and Eocene sequence yet recovered by deep sea drilling in the high latitudes of the Southern Ocean. The nannofossil-foraminifer oozes and chalks recovered from Maud Rise at 65°S in the Weddell Sea provide a unique opportunity for biostratigraphic study of extremely high southern latitude carbonate sediments.

The presence of warm water index fossils such as the discoasters and species of the *Tribrachiatus* plexus facilitate the application of commonly used low latitude calcareous nannofossil biostratigraphic zonation schemes for the upper Paleocene and lower Eocene intervals. In the more complete section at Site 690, Okada and Bukry Zones CP1 through CP10 can be identified for the most part with the possible exception of Zone CP3. Several hiatuses are present in the sequence at Site 689 with the most notable being at the Cretaceous/Tertiary and Paleocene/Eocene boundaries.

Though not extremely diverse, the assemblage of discoasters in the upper Paleocene and lower Eocene calcareous oozes is indicative of warm, relatively equable climates during that interval. A peak in discoaster diversity in uppermost Paleocene sediments (Zone CP8) corresponds to a negative shift in $\delta^{18}\text{O}$ values. Associated coccolith assemblages are quite characteristic of high latitudes with abundant *Chiasmolithus*, *Prinsius*, and *Toweius*. Climatic cooling is indicated for middle Eocene sediments by assemblages that contain very abundant *Reticulofenestra*, lack common discoasters and sphenoliths and are much less diverse overall.

Two new taxa are described, *Biscutum? neocoronum* n. sp. and *Amithalithina sigmundii* n. gen., n. sp.

INTRODUCTION

Ocean Drilling Program Leg 113 Sites 689 and 690 are located 700 km off east Antarctica on Maud Rise at latitude 65°S (Fig. 1A). The sites were cored to retrieve calcareous and siliceous sediments beneath the present day Antarctic water mass in order to study the changes in these sediments in response to the late Mesozoic-Cenozoic evolution of climate and ocean conditions around Antarctica. Of particular interest is the high percentage of nannofossil ooze and chalk recovered at this exceptionally high-latitude site, the southernmost locality to have yielded such sediments in the history of deep sea drilling.

Site 689 lies nearly 116 km northeast of Site 690, which is downslope on the southwest flank of Maud Rise as shown in the bathymetric profile in Figure 1B. At Site 689, siliceous and calcareous oozes to chalks were recovered to a depth of 297 mbsf (meters below seafloor). Cherts are present near the top of the Pliocene as well as in the Maestrichtian sequence. The Neogene section consists mostly of radiolarian and diatom oozes with minor interbeds of calcareous nannofossil ooze in the Miocene. Foraminifer-nannofossil oozes grading to chalks comprise the Paleogene to Maestrichtian sequence (Fig. 2).

Lithologies at Site 690 are similar except that there is less chert and a higher terrigenous component in the Paleocene and Maestrichtian sediments. In addition, the section has fewer hiatuses.

This study will consider the calcareous nannofossil biostratigraphy of the Paleocene to middle Eocene of Sites 689 and 690. See Wei and Wise (this volume) for studies of nannofossils from the middle Eocene to Miocene of these sites, and Pospichal and Wise (this volume, chapters 32 and 30) for the descrip-

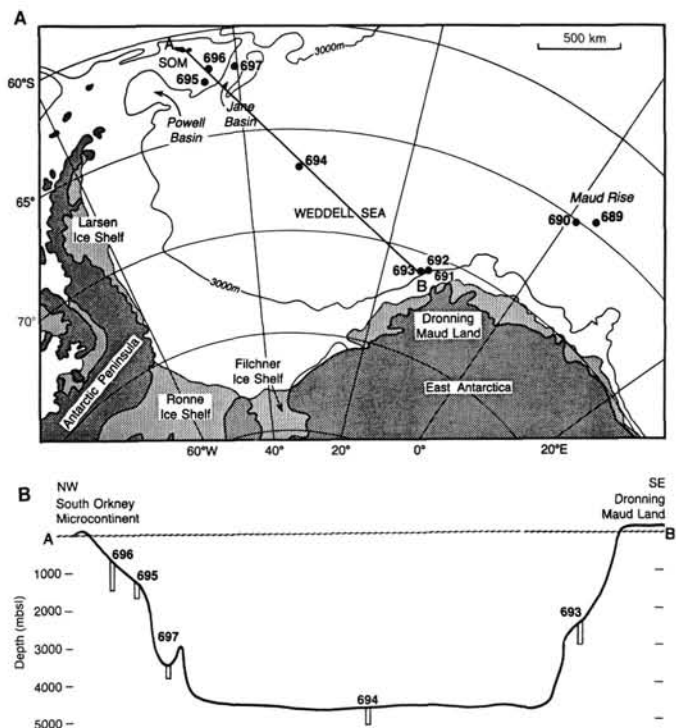


Figure 1. A. Location map of Sites 689, 690, and other ODP Leg 113 Sites, Weddell Sea off East Antarctica. SOM = South Orkney microcontinent. Bathymetric contours are numbered every 1000 m. B. Bathymetric profile of Maud Rise projected to the west (see A) along a schematic northwest-southeast transect across the Weddell Sea, showing the relative positions and depth distributions of the Leg 113 sites. mbsf = meters below sea level.

¹ Barker, P. F., Kennett, J. P., et al., 1990. *Proc. ODP, Sci. Results*, 113: Col- lege Station, TX (Ocean Drilling Program)

² Department of Geology, Florida State University, Tallahassee, FL 32306.

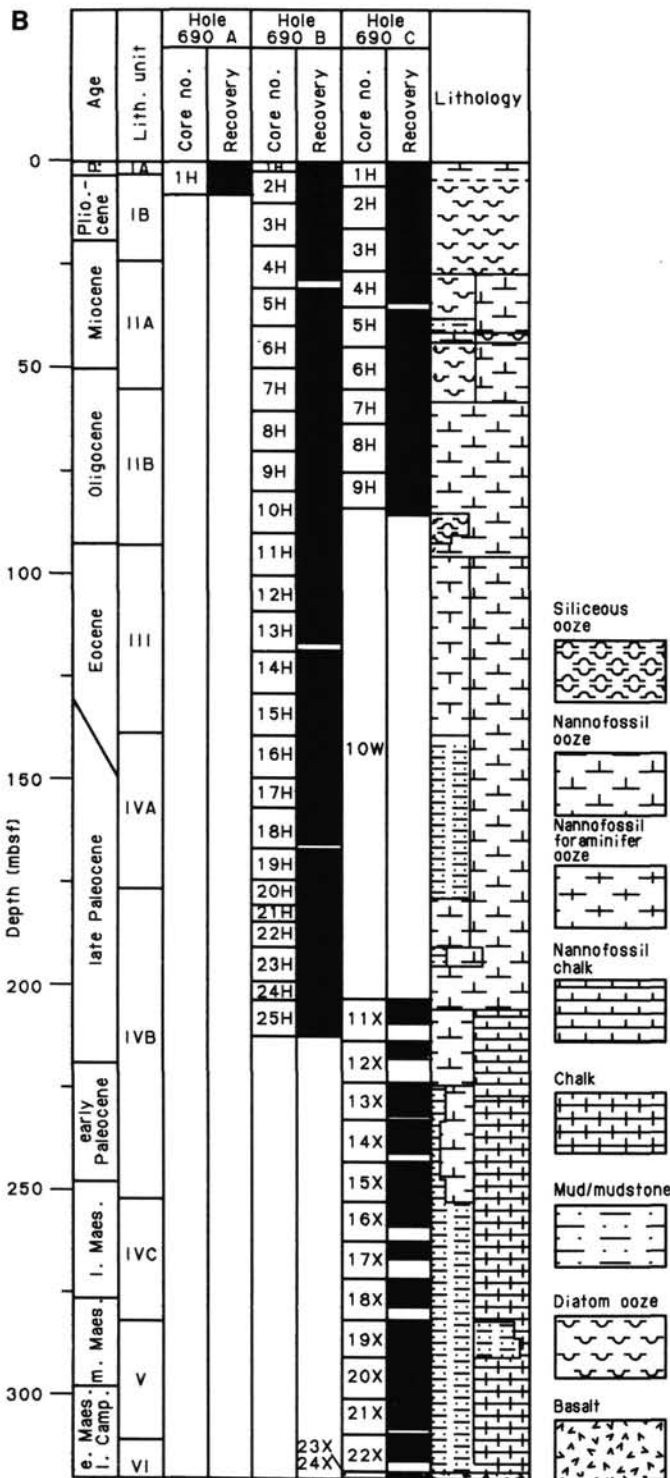


Figure 2 (Continued).

Relative individual species abundance estimations follow the procedure of Hay (1970) and are indicated in the following manner: V = very abundant (> 10 specimens/field of view); A = abundant (1–10 specimens/field of view); C = common (1 specimen/2–10 fields of view); F = few (1 specimen/11–100 fields of view); R = rare (1 specimen/101–1000 fields of view); P = present (only 1 specimen observed/slide).

ZONATION

The number-coded coccolith zonation compiled by Okada and Bukry (1980) is used with some modifications in this report for the Paleocene and Eocene sequences (Fig. 3, Tables 1–5). Although this zonation was developed primarily for the low latitudes, the nannofossil assemblages in the Paleocene and lower Eocene sections at this high-latitude site are sufficiently diverse to allow the application of this scheme. Most zones can be recognized in the Paleocene and lower Eocene, although in most cases, the higher biostratigraphic resolution obtained from sub-zone identifications cannot be achieved.

Paleocene

Diversity in the lower Paleocene is adequate to allow the identification of most zones and subzones except for the *Ellipsolithus macellus* Zone (CP3). That zone is based on the first occurrence (FO) of the nominate species, a low- to mid-latitude, relatively shallow-water form which is rare in many sections and is absent here. An alternate approach to approximate the CP2/CP3 boundary is the use of the FO of *Neochiastozygus saepes* or *Prinsius martinii* (Perch-Nielsen, 1979a). This usage is applied in this report to approximate the base of the zone at Site 690. The Cretaceous/Tertiary (K/T) boundary or the base of the *Zygodiscus sigmoides* Zone (CP1) is defined here on the FO of *Biantholithus sparsus* (Pospichal and Wise, this volume, chapter 32). This differs from the Okada and Bukry (1980) scheme, which uses the last Cretaceous species to mark the base of CP1. At Site 690, however, the original K/T boundary surface has been all but obliterated by strong bioturbation and several other criteria have been used to delimit that horizon (see Pospichal and Wise this volume, chapter 32).

The delineation of the upper Paleocene *Discoaster mohleri* Zone (CP6) is hampered by the sporadic occurrence of the warm-water species, *D. mohleri*, the FO of which marks the base of the zone. Thus, the CP5/CP6 boundary cannot be determined with a high degree of confidence.

Paleocene/Eocene Boundary

The presence of the *Tribrachiatus* plexus here allows for an accurate zonation of the lower Eocene. The Paleocene/Eocene boundary is marked in this report by the FO of *T. bramlettei*, which marks the NP9/NP10 boundary of Martini (1971). Traditionally, the Paleocene/Eocene boundary is drawn at the top of NP9, which roughly correlates to the top of CP8 of Okada and Bukry (1980), who mark the top of the zone by the FO of *T. contortus*. However, the first occurrence of this form is noted by most authors above the Paleocene/Eocene boundary (e.g., Hay and Mohler, 1967). The FO of *D. diastypus* is also used by Okada and Bukry (1980) to define this boundary, but the occurrence of this form is too rare in this section to be used as a reliable marker. The last occurrence (LO) of *Fasciculithus* was noted by Shackleton et al. (1984) to occur slightly below NP10 and could be used to approximate the boundary, except that here, because of reworking, its LO is well above the CP8/CP9 boundary and even above the LO of *T. contortus* (Table 3).

Diversity is noticeably lower in the middle Eocene, and the occurrence of warm-water marker species is sporadic. For this report it is necessary to combine the *Discoaster sublodoensis* (CP12) and *Nannotetrina quadrata* (CP13) Zones. Species such as *D. sublodoensis* and *Nannotetrina fulgens* were noted, but their occurrences were too inconsistent to be reliable markers. Usual markers for the middle Eocene, *Rhabdosphaera inflata*, *R. gladius*, *Chiasmolithus gigas*, and *D. saipensis*, were not noted in the section. Further observations on the biostratigraphy of Sites 689 and 690 are discussed below and summarized in

Table 1. Distribution of calcareous nannofossils in the Eocene of ODP Hole 689B. V = very abundant, A = abundant, C = common, F = few, R = rare, G = good, M = moderate, P = poor. Reworked specimens are denoted by lower case letters.

Age	Zone or subzone	Core, section, interval (cm)	Depth (mbsf)	Abundance	Preservation	<i>Amithalithina signundii</i>	<i>Biscutum? neocoronum</i>	<i>Biscutum</i> sp.	<i>Chiasmolithus bidens</i>	<i>C. expansus</i>	<i>C. solitus</i>	<i>Coccolithus formosus</i>	<i>C. pelagicus</i>	<i>Cyclicargolithus</i> sp. cf. <i>C. luminis</i>	<i>Discoaster barbadiensis</i>	<i>D. deflandrei</i>	<i>D. lenticularis</i>	<i>D. mediosus</i>	<i>D. mohleri</i>	<i>D. multiradiatus</i>	<i>D. nobilis</i>	<i>D. praebifax</i>	<i>D. sublodoensis</i>	<i>Discoaster</i> sp.	<i>Ellipsolithus distichus</i>	<i>E. lajollaensis</i>	<i>Fasciculithus involutus</i>	<i>F. tympaniformis</i>	Genus and species indet.	<i>Heliolithus univertus</i>	
middle Eocene	<i>Reticulofenestra umbilica</i> (CP14)	17H-6, 131-133	157.92	V M	F	A	P	A	R	
		17H, CC	158.80	V M	R	A	F	A	
		18H-1, 31-33	159.12	V M	F	A	P	A	R	
		18H-2, 31-33	160.62	V M	C	A	F	A	.	.	.	P	
		18H-3, 31-33	162.12	V M	C	A	.	A	
		18H-4, 31-33	163.62	V P	C	A	P	A	.	.	.	R	F	
	<i>Nannotetrina quadrata/ Discoaster sublodoensis</i> (CP13)/(CP12)	18H-5, 31-33	165.12	V P	.	P	.	.	.	C	A	F	A	.	.	P	C	
		18H-6, 31-33	166.62	V M	C	A	R	A	F	
		18H, CC	168.50	V M	F	A	R	A	.	P	F	.	.	p	.	.	
		19H-1, 30-32	168.81	V M	P	C	A	P	A	.	.	P	F	
		19H-2, 30-32	170.31	V M	P	C	A	.	A	F	
		19H-3, 30-32	171.81	V M	C	A	.	A	.	.	R	P	P	.	F	.	.	.	R	.	
		19H-4, 30-32	173.31	V M	C	A	P	A	p	C	.	
		19H-5, 30-32	174.81	V M	C	A	.	A	.	.	P	P	
		19H-6, 30-32	176.31	V M	C	A	.	A	.	P
		20H-1, 30-32	178.41	V M	P	C	A	.	A	R
		20H-2, 30-32	179.91	V M	C	A	.	A	P	.	P
		20H-3, 30-32	181.41	V M	F	A	.	A	P	.	R	P
		20H-4, 30-32	182.91	V M	F	A	.	A	F
		21H-1, 30-32	188.11	V M	F	A	.	A	.	P	.	F	F	.	p	.	.	.
		21H-2, 30-32	189.61	V M	F	A	.	A	.	.	P	F	P	.	P	.	.	p	.	.	.
		21H-3, 30-32	191.11	V M	F	A	.	A	R
21H, CC	197.50	V M	C	A	F	A	.	.	P	R	.	P	.	.		
22X-1, 29-30	197.80	V P	F	C	A	F	A	.	.	F	F	R		
22X-2, 27-29	199.28	V P	C	F	A	F	A	.	.	F	R	F	F	F	F	F	P	.		
22X-2, 132-133	200.33	V M	C	C	A	F	A	.	.	F	F	F	P		
22X-3, 30-32	200.82	V M	C	.	P	.	.	C	A	C	A	.	.	F	P	F	.	P	p	.	F	.		
22X-3, 132-133	201.83	V M	C	F	A	F	A	.	.	F	F		
late Paleocene	<i>Discoaster multiradiatus</i> (CP8)	22X-4, 30-32	202.31	V M	F	R	P	?	P	A	R	A	R	.	R	.	.	F	.	.	.	R	.	.	R	.	P	.	.		
		22X-5, 30-32	203.81	V M	.	F	.	C	P	A	.	F	.	.	.	F	F	.	C	F	P	.	.	.	
		22X-5, 130-132	204.88	V M	.	R	.	C	.	A	.	F	.	.	.	F	F	.	C	C	
		22X, CC	207.20	V M	.	F	A	A	.	A	.	C	F	?	A	A	.	.	

Figure 4, and Tables 1-5. Correlation of biostratigraphy with magnetostratigraphy is also shown in Figure 4.

SITE SUMMARIES

Site 689 (64°31.01' S, 03°05.99' E; water depth = 2080 m; Tables 1, 2)

Hole 689B was cored to a depth of 297 mbsf, where chert layers forced drilling to be terminated in Maestrichtian chalks an estimated 30 m above basement. Foraminifer-nannofossil oozes are present in the upper Eocene to upper Paleocene section, grading to chalk in the lower Paleocene at this site (Fig. 2A). Calcareous nannofossils are abundant in all samples and preservation is either poor or moderate (Tables 1, 2). As shown in Figure 4A, hiatuses were recorded at the Cretaceous/Tertiary boundary (Pospichal and Wise this volume, chapter 32), in the Danian, across the Paleocene/Eocene boundary, and in the upper Eocene/lower Oligocene (Wei and Wise, this volume).

Eocene

Sediments in Samples 113-689B-17H-6, 131-133 cm (157.92 mbsf), to -18H-4, 31-33 cm (163.62 cm), are placed in the *Reticulofenestra umbilica* Zone (CP14) based on the first consistent

occurrence of *R. umbilica*, which is never more than few in any samples examined. Diversity is quite low through this zone with the dominant species being abundant *Chiasmolithus solitus*, *Coccolithus pelagicus*, *R. samodurovii*, and *Zygrhablithus bijugatus*. Few to common *C. formosus*, *C. expansus*, and *Neococcolithes dubius* are present also.

Samples 113-689B-18H-5, 31-33 cm (165.12 mbsf), to -22X-3, 132-133 cm (201.82 mbsf), are assigned to the combined *D. sublodoensis*-*N. quadrata* Zones (CP12-CP13). The assemblage, as above, is dominated by *Reticulofenestra* spp. and *C. solitus*. *Neococcolithes dubius* is common to abundant throughout and rare *D. sublodoensis* are present in only a few samples near the base of the interval. No attempt was made here to separate Zones CP12 and CP13. A few specimens of the CP13 zonal marker, *N. fulgens* (= *N. quadrata*), were noted in Samples 113-689B-19H-1, 30-32 cm, and -19H-2, 30-32 cm, but its occurrence is too rare to be considered useful. *Amithalithina signundii* n. gen., n. sp. is common near the base of this zone.

A hiatus spanning Zones CP9 to CP11 separates this zone from upper Paleocene sediments of Zone CP8. This occurs between Samples 113-689B-22X-3, 132-133 cm, and -22X-4, 30-32 cm, and is indicated in Figure 4A by an arrow and a dashed line.

Table 2. Distribution of calcareous nannofossils in the Paleocene of ODP Hole 689B. Symbols as in Table 1.

Age	Zone or subzone	Core, section, interval (cm)	Depth (mbsf)	Abundance Preservation	<i>Biscutum castrorum</i>	B. ? neocoronum	<i>Biscutum</i> sp.	<i>Chiasmolithus bidens</i>	<i>C. danicus</i>	<i>Chiasmolithus</i> sp.	<i>Coccolithus cavus</i>	<i>C. pelagicus</i>	<i>C. sp. cf. C. pelagicus</i>	<i>Cruciplacolithus edwardsii</i>	<i>C. primus</i>	<i>C. tenuis</i>	<i>Cyclagelosphaera reinhardtii</i>	<i>Discoaster lenticularis</i>	<i>D. mediosus</i>	<i>D. mohleri</i>	<i>D. multiradiatus</i>	<i>D. praehifaj</i>	<i>Discoaster</i> sp.	<i>Ellipsolithus distichus</i>	<i>Fasciculithus involutus</i>	<i>F. tympaniformis</i>	<i>Fasciculithus</i> sp.	<i>Heliolithus cantabrigae</i>	<i>H. riedelti</i>	
late Paleocene	<i>Discoaster multiradiatus</i> (CP8)	23X-1, 29-31	207.50	V M	.	F	.	C	.	C	.	A	F	F	F	F	C	F	F	P	A	C	.	.	.	
		23X-2, 29-31	209.00	V M	.	F	P	A	.	A	.	A	F	.	R	C	.	.	.	C	C	.	.	.	
		23X-3, 29-31	210.50	V M	.	R	C	A	.	A	.	A	F	.	.	C	.	.	P	A	C	.	.	.	
		23X-4, 29-31	212.00	V M	.	F	C	A	.	A	.	A	R	.	F	R	.	F	C	A	.	.	.	
		23X, CC	216.90	V M	.	F	C	A	.	A	.	C	R	.	F	P	F	.	C	A	.	.	.	
		24X-1, 30-32	217.20	V M	.	.	C	A	.	A	.	A	F	F	.	.	P	A	C	.	.	.
	<i>Discoaster nobilis</i> (CP7)	24X-1, 116-118	218.06	V M	.	P	C	A	.	A	.	A	P	F	.	.	R	A	C	.	.	.	
		24X, CC	226.60	V M	.	F	C	A	.	A	.	C	R	C	C	.	.	F	
	early Paleocene	<i>Ellipsolithus macellus/Chiasmolithus danicus</i> (CP3)/(CP2)	25X-1, 18-19	226.78	V M	C	.	.	.	P	.	C	.	R	A	C	C
			25X-1, 81-82	227.41	V M	C	.	.	.	F	.	A	.	P	A	C	C	P	.	.
25X-2, 6-7			228.16	V M	F	.	.	.	F	.	.	.	P	A	C	A	
<i>Cruciplacolithus tenuis</i> (CP1b)		25X-2, 39-40	228.49	V M	C	.	.	.	?	.	A	.	C	A	A	A	
		25X-2, 72-73	228.82	V M	C	.	.	.	?	.	C	.	P	C	C	A	
		25X-3, 10-11	229.71	V M	C	C	.	F	C	C	A	
		25X-3, 67-68	230.28	V M	C	F	.	C	A	
		25X-4, 14-15	231.25	V M	C	P	.	F	A	A	
		25X-4, 70-71	231.81	V M	C	F	.	A	A	
		25X-5, 5-6	232.66	V M	C	A	A	P	
		25X-5, 40-41	233.01	V M	C	A	A	P	
		25X-5, 60-61	233.21	A M	C	C	C	
25X-5, 81-82	233.42	A M	F	P	F			

interval with abundant *Hornibrookina* preceding the FO of *C. tenuis* as at Site 690. In addition, no iridium anomaly was detected at this Cretaceous/Tertiary contact as was found at Site 690 (Michel et al., this volume). Thus the preponderance of the evidence suggests that Subzone CP1a is absent at Site 689. The K/T boundary is discussed in more detail in Pospichal and Wise (this volume, chapter 32).

Site 690 (65°09.63' S, 01°12.30' E; water depth = 2914 m; Tables 3-5)

Two holes drilled at Site 690 penetrated Paleogene sediments. Hole 690B was cored to a depth of 213.4 mbsf before bottoming out in the upper Paleocene *Heliolithus kleinpellii* Zone (CP5). Paleogene sediments consist of calcareous nannofossil ooze and foraminifer-nannofossil ooze. The section is much more complete through the Eocene and Paleocene at this site as the sequence is continuous from the middle Paleocene through the middle Eocene. A possible hiatus exists in the lower Paleocene of Hole 690C between Zones CP2 and CP4. In addition, the lower Eocene at this site, although apparently complete, is quite condensed when compared to the underlying Paleocene unit.

The Eocene and uppermost Paleocene sequence was washed through during the drilling of Hole 690C. In a successful attempt to overlap this hole with the basal sediments of Hole 690B, coring commenced at 204.2 mbsf in nannofossil oozes of late Paleocene age. Unfortunately, the overlapping Cores 113-690C-11X and -12X were highly disturbed and recovery was poor.

Hole 690C cored through the K/T boundary and reached basement at 317.0 mbsf where 1.71 m of basalt was sampled below the Maestrichtian nannofossil chalks. The lower Paleocene to Maestrichtian chalks contain a high terrigenous component in contrast to Site 689. The much improved coccolith preservation at Site 690 is most likely due, at least in part, to this added component.

As discussed in Pospichal and Wise (this volume, chapter 32), the K/T boundary at this site appears to be continuous. Although the interval is highly bioturbated, the identification of the boundary is aided by a strong color contrast between Cretaceous and Tertiary sediments. The dark brown color of the Tertiary material is most likely due to an increase in clay content, which is also noted at Site 689. Such an increase in clay content is present at many deep-sea K/T boundary sections and, in general, is attributed to a drop in calcareous plankton productivity. The following descriptions of Holes 690B and 690C are summarized in Figure 4B and Tables 3-5.

Hole 690B

Eocene

The combined *Discoaster subloadoensis*-*Nannotetrina quadrata* Zones (CP12-CP13) are present in Section 113-690B-12H, CC (108.5 mbsf), to Sample 113-690B-15H-3, 30-32 cm (131.41 mbsf). The FO of *D. subloadoensis* defines the base of this interval, and the top is placed at the FO of *Reticulofenestra umbilica*. This zonal assignment is hampered by the inconsistent occurrence of *D. subloadoensis* and the fact that *R. umbilica* has been observed previously within sediments of Zone CP13 (Perch-Nielsen, 1985; Applegate and Wise, 1987). In addition, specimens of the CP13 marker taxon, *Nannotetrina fulgens*, were observed at Hole 689B but not at the present site. The CP12/13 boundary is approximated by the LO of *D. lodoensis* in Sample 113-690B-14H-7, 27-29 cm (127.78 mbsf) but, considering its rare occurrence, the zonal boundary is drawn with a minimum of confidence. This is indicated by a dashed line shown in Figure 4B and Table 3. Sediments of these zones contain abundant *Chiasmolithus bidens*, *Zygrhablithus bijugatus*, *Coccolithus pelagicus*, *Neococcolithes dubius*, and *Reticulofenestra*. *Chiasmolithus expansus*, *Coccolithus formosus*, and *Amithalithina sigmundii* n. gen., n. sp. are common throughout this interval.

Table 2 (continued).

Age	Zone or subzone	Core, section, interval (cm)	<i>Gartnerago</i> spp.	<i>Kamptnerius magnificus</i>	<i>Lucionorhabdus</i> sp.	<i>Naphrolithus frequens</i>	<i>Prediscosphaera cretacea</i>	<i>P. spinosa</i>	<i>P. stoveri</i>	<i>Reinhardtites levis</i>
late Paleocene	<i>Discoaster multiradiatus</i> (CP8)	23X-1, 29-31	p	p	.	.	r	.	.	.
		23X-2, 29-31	p	.	.	.
		23X-3, 29-31	.	f
		23X-4, 29-31	.	p
		23X, CC	.	p
		24X-1, 30-32
late Paleocene	<i>Discoaster nobilis</i> (CP7)	24X, CC	.	f
		25X-1, 5-6	.	c	.	f	f	.	.	p
early Paleocene	<i>Ellipsolithus macellus/Chiasmolithus danicus</i> (CP3)/(CP2)	25X-1, 18-19	.	p	.	p	p	.	.	.
		25X-1, 81-82	p	f
		25X-2, 6-7
	<i>Cruciplacolithus tenuis</i> (CP1b)	25X-2, 39-40
		25X-2, 72-73	p	r	.	.	p	.	.	.
		25X-3, 10-11	.	f	.	.	p	.	.	.
		25X-3, 67-68	.	r	.	p
		25X-4, 14-15	.	f	.	r	r	.	.	.
		25X-4, 70-71	p	.	.	.	p	.	.	.
		25X-5, 5-6	.	f	.	p	f	.	.	.
25X-5, 40-41	p	.	.	f	f	.	.	.		
25X-5, 60-61	f	f	.	f	f	p	c	.		
25X-5, 81-82	f	c	p	a	c	f	a	.		

690B-25H, CC (213.4 mbsf), at the base of Hole 690B. Rare to common *H. kleinpellii*, *Neochiastozygus cearae*, *N. junctus*, *Hornibrookina australis*, *Biscutum? neocoronum* n. sp., and *Zygodiscus sigmoides* characterize the zone, as well as those forms listed above.

Hole 690C

After washing through to the Paleocene in Hole 690C, the first core taken, Core 113-690C-11X, had very poor recovery. Poor luck continued with Core 113-690C-12X as the core liner was shattered and the sediments within highly disturbed. The presence of *Discoaster multiradiatus* and *Heliolithus riedelii* in Core 113-690C-11X place it in the range of Zones CP7 and CP8. Core 113-690C-12X can be placed in Zones CP5-CP6 based on the presence of *Heliolithus kleinpellii* and *Discoaster mohleri*. It would appear from this that overlap had occurred between Holes 690B and 690C with both yielding sediments of Zone CP5. Unfortunately, continuous recovery across the CP4/CP5 boundary was not achieved.

Samples 113-690C-13X-1, 28-30 cm (223.89 mbsf), to -13X-4, 129-131 cm (229.40 mbsf), are assigned to the *Fasciculithus tympaniformis* Zone (CP4). The assemblage of this zone consists of abundant *Chiasmolithus danicus*, *Prinsius martinii*, and *P. dimorphosus*, and few to common *F. tympaniformis*, *Cruciplacolithus edwardsii*, *Thoracosphaera*, and *Hornibrookina teuriensis*. *Prinsius bisulcus* first occurs in this zone. The original site reports (Shipboard Scientific Party, 1988) indicate a hiatus encompassing Zone CP4, but with further investigation, rare to few specimens of the CP4 marker species, *F. tympaniformis* were observed down to the base of the above mentioned interval.

The short interval comprised of Samples 113-690C-13X-5, 129-131 cm (230.90 mbsf), and -13X-6, 28-30 cm (231.39 mbsf), is tentatively placed in the *Ellipsolithus macellus* Zone (CP3)

based on the presence of abundant *Prinsius martinii* and *Neochiastozygus saepes*. Also present in the interval are early forms of the genus *Fasciculithus*.

Section 113-690C-13X, CC (233.20 mbsf), to Sample 113-690C-14X-3, 28-30 cm (237.99 mbsf), are assigned to the *Chiasmolithus danicus* Zone (CP2). The zone is marked by abundant *C. danicus*, *Toweius selandius*, and *P. dimorphosus* plus common *Thoracosphaera*, *Biscutum castrorum*, *C. edwardsii*, and *Z. sigmoides*. *Cruciplacolithus tenuis* and *Hornibrookina teuriensis* are rare to few throughout the zone.

Samples 113-690C-15X-1, 2-3 cm (242.92 mbsf), to -15X-3, 151-152 cm (247.39 mbsf), are assigned to the *Cruciplacolithus tenuis* Subzone (CP1b). *Coccolithus cavus*, *Toweius selandius*, and *Thoracosphaera crassa* have their first occurrences in this interval. The zonal marker, *C. tenuis*, is the most abundant form along with *Zygodiscus sigmoides* and *Prinsius dimorphosus*. *Hornibrookina edwardsii* (Pospical and Wise this volume, chapter 32) is abundant at the base of this zone. In addition, reworked Cretaceous forms are common throughout the interval.

Samples 113-690C-15X-4, 1-2 cm (247.41 mbsf), to the Cretaceous/Tertiary boundary in the interval of Samples 113-690C-15X-4, 41 cm, to -15X-4, 49-50 cm (247.81-247.89 mbsf), are placed in the *Cruciplacolithus primus* (CP1a) Subzone. The zone is based on the interval from the FO of *Biantholithus sparsus* at the K/T boundary to the FO of *C. tenuis*. It should be noted that in this section, the FO of *C. primus* coincides with that of *C. tenuis* and does not precede it as reported from most other sections. This may be attributed to strong bioturbation or possibly a brief hiatus. Evidence in favor of such a hiatus is discussed in Pospical and Wise (this volume, chapter 32).

In addition to common Cretaceous forms, the assemblage of this subzone (CP1a) is dominated by few to common opportunistic "survivor" forms such as *Zygodiscus sigmoides*, *Markalius inversus*, *Neocrepidolithus*, *Thoracosphaera*, and *Biscutum castrorum* (*B. constans* of some authors). However, *Hornibrookina edwardsii*, which appears in this interval, dominates the assemblage near the top of this zone. The FO of *Biantholithus sparsus* was noted in burrowed sediments of Sample 113-690C-15X-4, 49-50 cm, where one specimen was detected in the SEM. Several specimens were observed in Sample 113-690C-15X-4, 43-44 cm. Considering the high degree of bioturbation, the K/T boundary is placed at Sample 113-690C-15X-4, 41.5 cm (247.815 mbsf), at the top of the highest undisturbed Cretaceous sediment (see discussion on bioturbation in Pospical and Wise this volume, chapter 32).

MAGNETOBIOSTRATIGRAPHY

Figure 4 provides a correlation of the calcareous nannofossil biostratigraphy of Sites 689 and 690 discussed above with the magnetostratigraphy of Hamilton (this volume) whose data encompass the Maestrichtian and lowermost Paleocene, and of Spieß (this volume), who analyzed the remaining Cenozoic section. Unfortunately, polarity of the sediments could not be determined for the Paleocene and lower middle Eocene in Hole 689B. Likewise, in Hole 690C, polarity was not determinable for the crucial interval encompassing Zones CP2 to CP4. The standard magnetostratigraphy of Berggren et al. (1985) is used here as reference for comparison of polarity patterns.

In Hole 689B, the CP13/14 boundary, which is based here on the first occurrence of *Reticulofenestra umbilica*, is placed near the top of Subchron 19R. Berggren et al. (1985) would place this boundary in Subchron 18R. Our data here are in close agreement with the data compilation by Wei and Wise (1989), who have shown that *R. umbilica* first appears no higher than Chron 19R in several South Atlantic sites and at the Contessa and Bottaccione sections. In Hole 690B, Spieß (this volume) has combined Chrons 19 and 20, therefore, it cannot be determined

exactly where the CP13/14 boundary falls. We place the boundary no higher than Chron 19 despite the difficulty in determining the first occurrence of *R. umbilica* at this site.

In Hole 690B, we estimate the CP12/13 boundary to be within Subchron 21R. The usual markers for this zonal boundary, *Nannotetrina fulgens* and/or *Rhabdosphaera inflata*, were not observed. Instead, we approximated this level on the disappearance of *Discoaster lodoensis* and *D. kuepperi*, whose last occurrences are generally noted to fall below this boundary. Hence, it is understandable that our simple estimation places the CP12/13 boundary too low when compared with the time-scale of Berggren et al. (1985) and with the data of Wei and Wise (1989). The latter authors show that the FO of *N. fulgens* (CP12/13 boundary) consistently lies within Subchron 21N at various localities.

The FO of *Discoaster sublodoensis* marks the CP11/12 boundary. This boundary falls within Subchron 22N in Hole 690B, which is in close agreement with Berggren et al. (1985), who correlate the boundary to the base of this subchron. Zones CP10 and CP11 are combined in this report, and the short section assigned to these zones spans the Subchron 22N/22R boundary. Berggren et al. would correlate Zone CP10 to Chron 23, which is below our placement here. Using the FO of *D. lodoensis*, we locate the CP9/CP10 boundary within Subchron 22R, which, as mentioned above, is about one chron higher than its position in the time scale of Berggren et al. (1985).

The Paleocene/Eocene boundary, according to the Berggren et al. (1985) time scale, falls within Subchron 24R. This level roughly corresponds to the CP8/CP9 boundary, which in Hole 690B, is located in Subchron 24N. The FO of *Tribrachiatum bramlettei* is used here to define this boundary, however a diachronous occurrence of this species, which is rare in this section, may contribute to the discrepancies here in correlations with magnetostratigraphy. The problems of using this form to mark this boundary are discussed in detail in Backman (1986).

The CP7/CP8 boundary is defined by the FO of *Discoaster multiradiatus*, which is near the top of Subchron 25N in Hole 690B. This is in agreement with data compilations of Wei and Wise (1989) and with the Berggren et al. (1985) scheme. As previously discussed, the CP5/CP6 boundary was not easily determined in Hole 690B. However, we have estimated that this horizon falls within Subchron 25R, which also closely agrees with the findings of the above-mentioned authors.

Continuous recovery was not achieved across the CP4/CP5 boundary as Hole 690B bottomed out in Zone CP5 (Subchron 26N). Overlapping cores in Hole 690C were disturbed and recovery was poor, hence magnetic data were unreliable. Polarity for sediments of Zones CP2–CP4 in Hole 690C also could not be determined.

Hamilton (this volume) was able to determine the magnetic polarity for sediments of the lowermost Paleocene Zone CP1 and of the Cretaceous/Tertiary boundary interval. The Subzone CP1a/CP1b boundary falls within Subchron 29N in Hole 690C, which is in agreement with most authors' findings as well as the scheme of Berggren et al. (1985). The K/T boundary itself lies just within Subchron 29R, also in accord with results from other localities (Alvarez et al., 1977; Thierstein, 1982).

DISCUSSION

Genus *Hornibrookina*

From New Zealand sections, Edwards (1973) first described the form, *Hornibrookina teuriensis*, with a known range starting in CP2. Perch-Nielsen (1977) later described *H. edwardsii* from DSDP Site 356 in the Southwest Atlantic, where its first occurrence is also placed at the base of CP2. In the Southeast Atlantic, Percival (1984) did not report *Hornibrookina* in Da-

nian sediments of the Walvis Ridge. Recently, Angelozzi (1988) reported the presence of both *H. edwardsii* and *H. teuriensis* in a mid-latitude, land-based section in Argentina, which she placed in Zone NP3 (CP2). However, in that section, she noted the first occurrence of *H. teuriensis* below that of *H. edwardsii*. In detailed studies from the North Sea and sections in Turkey, Varol (1989) noted the first occurrence of *H. edwardsii* also near the base of CP2. In Maud Rise sediments, we observed the first occurrence of *H. edwardsii* in CP1a with *H. teuriensis* appearing shortly after that in CP1b. Overall, the genus *Hornibrookina* has been previously reported this low in the section only by Jiang and Gartner (1986), based on their light microscope study of the Brazos River section in Texas, but they identify the form as *H. teuriensis*.

Particularly unexpected at Site 690 is the dominance of *H. edwardsii* in this assemblage at the CP1a/1b boundary, where it comprises 45% of the assemblage (see table 1 of Pospichal and Wise, this volume, chapter 32). This appears to be a highly provincial phenomenon, and it would be interesting if the same phenomenon is noted in the austral high-latitude sections of ODP Legs 114, 119, and 120. For further description of *Hornibrookina* see Systematic Paleontology section of Pospichal and Wise (this volume, chapter 32).

Genus *Fasciculithus*

In regards to the placement of the CP3/CP4 boundary in Hole 690C, *Fasciculithus tympaniformis* is not the first *Fasciculithus* to appear. As mentioned above, several precursor forms of the species are noted in the zone below but the base of Zone CP4 is based here on the FO of forms positively identified as *F. tympaniformis*. This is largely a subjective determination and possibly a more viable method would be to draw the boundary at the FO of the genus *Fasciculithus*. This interpretation would drop the boundary down to the level where we have drawn the CP3/CP2 boundary, thus eliminating Zone CP3. In view of the data in Table 3, a hiatus encompassing CP3 is entirely possible. The sudden appearance of *Prinsius martinii* and *Neochiastozygus saepes* in high numbers along with the sudden disappearance of *Toweius selandius* in Sample 113-690C-13X-6, 28–30 cm, may be cited as partial evidence for such a hiatus, although the evidence is not at all conclusive. As we have no other sections for comparison from this high southern latitude, the sequence of events involving nannofossil assemblages of Zones CP3 and CP4 remains unclear.

The last occurrence of *Fasciculithus* is likewise difficult to determine in this section. We have observed common reworked forms throughout the lower Eocene although its last occurrence is generally noted to coincide with the Paleocene/Eocene boundary.

Genus *Tribrachiatum*

Another unexpected finding at this high-latitude, deep-sea section, is the presence of *Tribrachiatum bramlettei* and *T. contortus*. These forms are generally thought to occur preferentially along continental margins. However, their presence here, although not in great abundance, would suggest that the forms did occupy open-ocean environments but were not preserved in deeper marine sediments. Maud Rise, which is quite remote from the Antarctic continental margin, apparently was shallow enough to allow preservation of these early forms of *Tribrachiatum*. In addition, their presence at this high latitude is indicative of a relatively warm early Eocene ocean as discussed below.

Discoasters, Sphenoliths, and Surface Ocean Conditions

Discoasters and sphenoliths are reliable indicators of warm surface waters (Bukry, 1973; Wei and Wise, 1989), and relatively warm surface-water conditions at a latitude of 65°S during the Paleocene and early Eocene is suggested by their presence in the

Table 3. Distribution of calcareous nannofossils in the Eocene of ODP Hole 690B. Symbols as in Table 1.

Age	Zone or subzone	Core, section, interval (cm)	Depth (mbsf)	Abundance	Preservation	<i>Amithalithina signunaii</i>	<i>Biscutum? neocoronum</i>	<i>Biscutum</i> sp.	<i>Chiasmolithus bidens</i>	<i>C. consuetus</i>	<i>C. eograndis</i>	<i>C. expansus</i>	<i>C. solitus</i>	<i>Coccolithus formosus</i>	<i>C. pelagicus</i>	<i>Cyclicargolithus</i> sp. cf. <i>C. luminis</i>	<i>Discoaster barbadiensis</i>	<i>D. sp. cf. D. bifax</i>	<i>D. deflandrei</i>	<i>D. diastypus</i>	<i>D. elegans</i>	<i>D. kuepperi</i>	<i>D. sp. cf. D. kuepperi</i>	<i>D. lenticularis</i>	<i>D. lodoensis</i>	<i>D. mediosus</i>	<i>D. megastypus</i>	<i>D. mohleri</i>	<i>D. multiradiatus</i>	<i>D. subloadoensis</i>
middle Eocene	<i>Reticulofenestra umbilica</i> (CP14)	12H-6, 130-132	107.61	V M	P	.	P	C	.	.	C	A	R	A	.	.	.	F
		12H-7, 29-31	108.10	V M	.	.	.	C	.	.	C	A	R	A	.	.	.	F
	<i>Nannotetrina quadrata</i> (CP13)	12H, CC	108.50	V M	.	.	.	F	.	.	.	C	A	R	A	.	.	P	F
		13H-1, 29-31	108.80	V M	.	.	.	F	.	.	.	C	A	R	A	.	.	.	R
		13H-2, 30-32	110.31	V M	.	.	.	C	.	.	.	C	A	R	A	.	.	.	F
		13H-3, 30-32	111.81	V M	.	.	.	C	.	.	.	C	A	R	A	.	.	.	R
		13H-4, 28-30	113.30	V M	.	.	.	C	.	.	.	C	A	R	A	.	.	.	R
		13H-5, 130-132	115.81	V M	P	.	.	C	.	.	.	C	A	R	A	.	.	.	R	F	F
		13H-6, 29-31	116.30	V M	.	.	.	P	C	.	.	F	A	R	A	.	.	.	F	F
		13H-7, 28-30	117.79	V M	.	.	.	C	.	.	.	C	A	R	A	.	.	.	R
		13H, CC	118.50	V M	.	.	.	C	.	.	.	C	A	R	A	.	.	.	P	R	F
		14H-1, 130-132	119.81	V M	.	.	.	C	.	.	.	C	A	R	A	.	.	.	R	F
		14H-2, 130-132	121.31	V M	.	.	.	C	.	.	.	C	A	R	A	.	.	.	R	R
		14H-3, 130-132	122.81	V M	F	.	.	C	.	.	.	C	A	R	A	.	.	.	R	F	R
14H-4, 130-132	124.31	V M	F	.	.	C	.	.	.	C	A	R	A	.	.	.	R	F	F	R		
14H-5, 130-132	125.81	V M	C	.	.	A	.	.	.	C	A	R	A	.	.	.	R	R	C	.	.	.	P	C		
14H-6, 130-132	127.31	V M	C	.	.	C	.	.	.	C	A	R	A	.	.	.	R	C		
early Eocene	<i>Discoaster sublodoensis</i> (CP12)	14H-7, 27-29	127.78	V M	C	R	R	A	.	.	C	A	R	A	.	.	F	F	F	C	
		14H, CC	128.10	V M	C	.	F	A	.	.	.	C	A	R	A	.	.	F	F	F	.	F	?	
		15H-1, 30-32	128.41	V M	C	.	.	A	.	.	.	C	A	R	A	.	.	.	F	F	F	
		15H-2, 30-32	129.91	V M	C	.	R	A	.	.	.	F	C	A	R	A	.	.	F	F	F	
	<i>Discoaster lodoensis/Tribraclhiatus orthostylus</i> (CP11)-(CP10)	15H-3, 30-32	131.41	V M	C	.	.	A	.	.	F	C	A	R	A	.	.	F	.	.	.	R	.	F	R	
		15H-4, 30-32	132.91	V M	F	.	.	A	.	.	.	C	A	R	A	.	.	R	.	.	.	?	.	R	.	.	.	p		
	<i>Discoaster diastypus</i> (CP9)	15H-5, 30-32	134.41	V M	C	.	F	A	.	.	A	C	A	R	A	.	.	C	R	.	C	.	.	R	
		15H-6, 30-32	135.91	V M	R	.	C	A	P	.	.	A	F	A	R	A	.	.	P	F	?	
		15H-7, 30-32	137.41	V M	R	R	A	A	.	.	.	A	C	R	A	A	R	
		15H, CC	137.80	V M	.	.	A	A	R	.	.	C	P	A	R	A	R	.	F	.	C	R		
16H-1, 28-30		138.09	V M	.	.	C	A	.	.	.	C	.	A	R	A	F	R	.	.	.	R			
16H-2, 28-30		139.59	V M	.	R	F	A	F	.	.	F	.	.	A	C	F	C			
16H-3, 28-30		141.09	V M	.	.	F	A	R	.	.	F	.	.	A	C	F			
16H-4, 28-30		142.59	V M	.	R	F	A	.	.	.	C	.	C	A	R	F	.	F				
16H-5, 28-30		144.09	V M	.	F	C	A	.	.	.	C	.	C	A	R	F	.	F			
16H-6, 28-30		145.59	V M	.	.	C	A	R	.	.	C	.	C	A	R	R	.	.	.	F			
16H-6, 130-132		146.61	V M	.	F	C	A	.	.	.	F	.	C	A	R	R	F	.	.	F				
16H-7, 28-30		147.09	V M	.	R	C	A	.	.	.	F	.	C	A	R	.	.	.	P	R	.	R	R	.	F	R	F			
16H, CC	147.50	V M	.	F	C	C	.	.	.	F	.	.	A	R	.	.	F	P	.	.	R	.	.	.	R	F				

sediments of Maud Rise. Although discoaster and sphenolith diversity is low, species such as *D. multiradiatus* and *S. moriformis* are quite abundant through much of the upper Paleocene sequences. Intervals of higher discoaster diversity such as in Samples 113-690B-17H-7, 28-30 cm, and -19H-3, 29-31 cm, should be indicative of the migration of this group southward during periods of warming. *Discoaster megastypus*, *D. mohleri*, and *D. mediosus* sporadically occur throughout the upper Paleocene section (usually in the same intervals) while *D. lenticularis* and *D. multiradiatus* are consistently present (Table 4). The sphenolith diversity is much less with only three species present. *S. moriformis* is quite abundant in the Paleocene and lower Eocene and is joined by very rare *S. radians* in a few samples in Zone CP12 of Hole 690B (Table 3). Few species of *S. editus* are also present in lower to middle Eocene samples.

The peak in discoaster diversity in Core 113-690B-19H is coincident with a negative shift in $\delta^{18}O$ values and a notable ^{13}C shift (Kennett and Stott, this volume; Stott et al., this volume). In addition, a major extinction of benthic foraminifers is noted in the same horizon (Thomas, this volume).

The numbers of discoasters decline sharply in the lower to middle Eocene sections. *Discoaster lodoensis* and *D. sublodoensis* are rare to few, and a small version of *D. barbadiensis* is very rare. Nondescript forms of the *D. deflandrei* group are consistently present as well. The disappearance of *D. sublodoensis* and the absence of an assemblage with *D. barbadiensis* and *D. saipanensis* in middle Eocene sediments of Maud Rise coincides with the beginning of the well documented global cooling trend at this time in addition to the deterioration of Antarctic climate (Shackleton and Kennett, 1975; Oberhänsli et al., 1984). At the same time the percentage of sphenoliths in Maud Rise samples also declines. *Sphenolithus moriformis* is quite abundant in lower Eocene Zones CP9-CP11 but not nearly as abundant in samples above these zones (Tables 1, 3). In the middle and lower latitudes, sphenoliths diversified. However, because of the above-mentioned cooling trend, these diverse assemblages apparently never had the opportunity to develop in the region of Maud Rise.

Despite the presence of several forms from the discoaster group, the upper Paleocene and lower Eocene assemblages of

Table 5. Distribution of calcareous nannofossils in the Paleocene of ODP Hole 690C. Symbols as in Table 1. In Sample 113-690C-15X-4, 43-44 cm, specimens of *Biantholithus sparsus*, denoted by a lower case letter, are interpreted to have been displaced downward by bioturbation.

Age	Zone or subzone	Core, section, interval (cm)	Depth (mbsf)	Abundance Preservation	<i>Amithalithina sigmundii</i>	<i>Biantholithus sparsus</i>	<i>Biscutum castrorum</i>	<i>B. ? neocoronum</i>	<i>Biscutum</i> sp.	<i>Braarudosphaera</i> sp.	<i>Chiasmolithus bidens</i>	<i>C. californicus</i>	<i>C. consuetus</i>	<i>C. danicus</i>	<i>C. eograndis</i>	<i>Chiasmolithus</i> sp.	<i>Coccolithus cavus</i>	<i>C. pelagicus</i>	<i>C. sp. cf. C. pelagicus</i>	<i>Cruciplacolithus edwardsii</i>	<i>C. primus</i>	<i>C. tenuis</i>	<i>Cyclagelosphaera reinhardtii</i>	<i>Cyclicargolithus</i> sp. cf. <i>C. luminitis</i>	<i>Discoaster</i> sp. cf. <i>D. falcatus</i>	<i>D. lenticularis</i>	<i>D. mohleri</i>	<i>D. multiradiatus</i>	
late Paleocene	(Poor Core Recovery) (CP5-8)	11X-1, 67-68	204.88	V M	.	.	F	F	.	A	.	P	.	F	C	.	A	.	.	.	P	.	C	F	F	.	F		
		11X-2, 31-32	206.02	V M	.	.	.	C	C	.	A	F	.	.	F	A	.	A	F	.	
		11X-3, 108-109	208.29	V M	F	.	F	F	F	P	A	A	.	P	F	.	
		11X-4, 51-52	209.22	V M	F	.	F	F	F	.	A	A	.	A
		12X-1, 30-32	214.21	V M	.	.	F	F	F	.	A	A	.	C
		12X-2, 132-134	216.73	V M	C	.	F	R	.	.	A	A	.	F
12X-3, 25-27	217.16	V M	.	.	.	C	.	.	A	P	A	.	F	P	P	P	.		
early Paleocene	<i>Fasciculithus tympaniformis</i> (CP4)	13X-1, 28-30	223.89	V M	.	.	.	P	C	.	C	.	.	A	.	A	.	C	.	F	.	R	
		13X-1, 129-130	224.90	V M	C	.	?	.	.	A	.	A	.	R	.	R
		13X-2, 129-130	226.40	V M	C	.	?	.	.	A	.	A	.	C	.	C	.	F
		13X-3, 129-131	227.90	V M	.	P	F	.	C	A	.	A	.	C	.	.	.	P	F
		13X-4, 129-131	229.40	V M	.	.	F	.	C	A	.	A	.	C	.	.	.	P	R
	<i>Ellipsolithus macellus</i> (CP3)	13X-5, 129-131	230.90	V M	.	.	C	.	F	A	.	A	.	C	.	F	.	P	R
		13X-6, 28-30	231.39	V M	.	.	A	.	F	A	.	A	.	C	.	C	.	F	P
	<i>Chiasmolithus danicus</i> (CP2)	13X, CC	233.20	V M	.	.	C	.	R	A	.	A	.	C	.	F	.	F	R
		14X-1, 28-30	233.49	V M	A	.	A	.	F	.	C	.	F
		14X-1, 126-130	234.48	V M	.	P	C	.	F	A	.	A	.	F	R	C	.	F	P
		14X-2, 28-30	234.99	V M	.	.	C	C	.	A	.	F	P	A	.	P
		14X-2, 126-130	235.98	V M	.	.	C	C	.	?	.	F	R	A	P	R
14X-3, 28-30	236.49	V M	.	.	C	F	.	?	.	F	F	A	R	R		
<i>Cruciplacolithus tenuis</i> (CP1b)	15X-1, 2-3	242.93	V M	.	.	C	P	C	.	F	C	A	
	15X-1, 85-86	243.76	V M	.	.	F	P	R	.	F	C	A	
	15X-2, 8-9	244.49	V M	.	.	C	R	F	.	C	F	A	
	15X-2, 87-88	245.28	V M	.	.	C	F	.	.	F	A	
	15X-3, 7-8	245.98	V M	.	.	F	P	P	.	F	A	
	15X-3, 80-81	246.71	V M	.	.	C	P	.	.	F	A	P	
	15X-3, 118-120	247.09	A M	.	.	C	F	A	
	15X-3, 151-152	247.41	A M	.	.	C	R	P	
<i>Cruciplacolithus primus</i> (CP1a)	15X-4, 1-2	247.42	A M	.	P	C	P	
	15X-4, 29-30	247.70	A M	.	.	C	
late Maestrichtian	<i>Nephrolithus frequens</i>	15X-4, 43-44	247.84	A M	.	f	C	

near the lower/middle Eocene boundary. It is interesting to note that on a global basis, hiatuses, disconformities, and/or relative sea-level falls have been recorded in several continental margin and deep-sea sections near the lower/middle Eocene boundary (e.g., Barr and Berggren, 1981; Poag et al., 1985; Olsson et al., 1988), and Vail et al. (1977) and Haq et al. (1987) have suggested that one of the most important sea-level falls occurred near this boundary as a result of eustatic lowering. The condensed or truncated section near the early/middle Eocene boundary on Maud Rise, therefore, may be tied to a global rather than to a merely local sedimentation pattern.

SYSTEMATIC PALEONTOLOGY

Genus *AMITHALITHINA* Pospical and Wise, n. gen. (Pl. 5, Fig. 3)

Type species. *Amithalithina sigmundii* Pospical and Wise, n.sp.

Diagnosis. Birefringent, elliptical to subround coccoliths comprised of two shields and a massive, high-standing central column nearly equal in width to the shields and composed of slightly inclined and imbricate lath-shaped elements.

Description. See characteristics of type species.

Remarks. Due to the high central column, specimens are frequently observed in side view. Due to the thick central column, specimens exhibit a high order (yellow) interference color in plan or side view. The name is from the Greek meaning "cake of stone."

Differentiation. The overall morphology of subround specimens superficially resembles some species of *Bomolithus* Roth (1973) and *Heliolithus* Bramlette and Sullivan (1961), but differs in that the outer cycle of elements of the central column of *Amithalithina* are distinctly inclined whereas those of the other genera rise vertically from the base. In addition, the shields of *Bomolithus* are not birefringent in plan view. In plan view, *Amithalithina* also resembles the genus *Pyrocyclus* Hay and Towe (1962), but the latter genus does not possess a very high central column and lacks the additional shield separating the central column from the proximal shield.

Amithalithina sigmundii Pospical and Wise, n. sp. (Pl. 5, Fig. 3)

Diagnosis. Medium to small subround to elliptical species of *Amithalithina* composed of two shields surmounted by a massive, flat topped central column composed of two cycles of elements about a hollow center.

Table 5 (continued).

Age	Zone or subzone	Core, section, interval (cm)	<i>Acuturris scotus</i>	<i>Ahmuelerella octaradiata</i>	<i>Arkhangelskiella cumbiformis specillata</i>	<i>Biscutum magnum</i>	<i>Chiasozygus</i> sp.	<i>Cretarhabdus conicus</i>	<i>Cribrosphærella daniae</i>	<i>C. ehrenbergii</i>	<i>Eiffelithus turrisseiffeli</i>	<i>Gartnerago</i> spp.	<i>Kampinerius magnificus</i>	<i>Lucianorhabdus</i> sp.	<i>Micula decussata</i>	<i>Nephrolithus frequens</i>	<i>Prediscosphaera cretacea</i>	<i>P. spinosa</i>	<i>P. stoveri</i>	
late Paleocene	(Poor Core Recovery) (CP5-8)	11X-1, 67-68	p	.	.	.	p	.	p	
		11X-2, 31-32	r	
		11X-3, 108-109	p	.	f	c	c	.	p	.	.	.	
		11X-4, 51-52	.	.	p	p	
		12X-1, 30-32	r	
		12X-2, 132-134	p	p	
		12X-3, 25-27	.	.	f	f	.	f	.	.	.	p	.	
		early Paleocene	<i>Fasciculithus tympaniformis</i> (CP4)	13X-1, 28-30	.	.	r	r
				13X-1, 129-130	r
				13X-2, 129-130	f	.	f	f	.	.	f
13X-3, 129-131	f			.	f	p	
<i>Ellipsolithus macellus</i> (CP3)	13X-4, 129-131		.	.	p	p	p		
	13X-5, 129-131		.	.	p	p	p		
<i>Chiasmolithus danicus</i> (CP2)	13X-6, 28-30		.	.	f	f		
	13X, CC		r	.	f	f	.	f	.	
	14X-1, 28-30		.	.	f	f	p	f	.	.	.	f	.	
	14X-1, 126-130		f	p	f	.	.	r	.	.	f	.	f	.	.	p	.	f	.	
	14X-2, 28-30	r	p	f	r	.	f	.	p	p	.	r	.		
	14X-2, 126-130	p	.	f	f	.	f	.	.	p	.	r	.		
late Maestrichtian	<i>Nephrolithus frequens</i>	14X-3, 28-30	p	.	f	.	.	p	p	p	.	p	.	.	.	p	.			
		15X-1, 2-3	.	.	p	r	r	.	.	p	.	r	
		15X-1, 85-86	.	.	p	f	p	
		15X-2, 8-9	p	.	f	.	.	.	f	p	p	.	f	p	.	p	.	.	.	
		15X-2, 87-88	p	.	f	r	.	
		15X-3, 7-8	.	.	p	p	p	.	.	p	.	.	
		15X-3, 80-81	.	.	f	p	f	.	r	f	.	f	
		15X-3, 118-120	.	r	c	.	r	.	f	r	r	.	c	.	.	c	c	.	c	
		15X-3, 151-152	f	r	.	.	.	p	f	p	f	.	c	.	.	c	c	.	a	
		<i>Cruciplacolithus primus</i> (CP1a)	15X-4, 1-2	f	f	c	.	p	f	f	p	f	f	c	p	.	c	c	p	c
15X-4, 29-30	f		.	c	.	f	f	f	f	f	f	c	p	p	c	c	r	a		

distal shield displays a low order of birefringence. The outer rim of the central area is quite bright, and the inner portion exhibits a thin extinction pattern. The species is most distinct in phase contrast light. The broad shield is dark in contrast to the bright outer rim of the relatively small central area. The inner portion of the central area is dark in phase contrast light, similar to that of the Mesozoic form *B. coronum* Wind and Wise (1977), from which the name is derived. In the SEM, the central area is composed of an outer rim of non-imbricate, blocky elements which surround the inner portion of the central area to form a small cavity.

Remarks. The species name is derived from that of the Campanian-Maestrichtian form, *Biscutum coronum*, because of its similarities in size and appearance in phase contrast light. The two species are distinct in cross polarized light. There is, however, a considerable stratigraphic gap between the ranges of the two taxa encompassing the middle to upper Maestrichtian plus the lower Paleocene Zones CP1-CP4. This species is the largest member of this genus in Paleocene and lower Eocene sediments of Maud Rise.

Occurrence. The species is few to common in upper Paleocene Zones CP5-CP8 and few to rare in lower Eocene Zones CP9-CP12 at ODP Leg 113 Maud Rise Sites 689 and 690 in the Weddell Sea. If this is a true *Biscutum*, then this occurrence considerably extends the range of this ge-

nus, which was formerly thought to have become extinct in the early Paleocene.

Size. The taxon ranges from 6 to 10 μm in length with the average around 7 or 8 μm. The holotype is 7 μm.

Holotype. Plate 1, Figure 1a.

Isotype. Plate 1, Figure 1b-d.

Type locality. Ocean Drilling Program Sample 113-690B-17H-7, 28-30 cm.

ACKNOWLEDGMENTS

This paper was excerpted from a thesis by J. Pospical submitted in partial fulfillment of the Master of Science degree at Florida State University in 1989. We thank our Leg 113 collaborators for helpful discussions. We are also grateful to Drs. David K. Watkins and Marie-Pierre Aubry for their helpful comments. We thank Professor Leon Golden of the F.S.U. Classics Department for assistance in formulating scientific names. The photomicrograph in Figure 11, Plate 3, was taken by Daniel Clay Kelly as a part of a nannofossil class project. The study was supported by National Science Foundation grant DPP-8414268,

Okada and Bukry (1980)

Martini (1971)

Datums
(This Report)

Eocene	CP15	<i>D. barbadiensis</i>	CP15b	<i>I. recurvus</i>	19/20	
			CP15a	<i>C. oamaruensis</i>	NP18	
	CP14	<i>R. umbilica</i>	CP14b	<i>D. saipanensis</i>	NP17	
			CP14a	<i>D. bifax</i>	NP16	└ <i>R. umbilica</i>
	CP13	<i>N. quadrata</i>	CP13c	<i>C. staurion</i>		
			CP13b	<i>C. gigas</i>	NP15	
			CP13a	<i>D. strictus</i>		
	CP12	<i>D. sublodoensis</i>	CP12b	<i>R. inflata</i>	NP14	└ <i>D. lodoensis</i> └ <i>D. kuepperi</i>
			CP12a	<i>D. kuepperi</i>		└ <i>D. sublodoensis</i>
	CP11	<i>D. lodoensis</i>			12/13	└ <i>D. lodoensis</i>
CP10	<i>T. orthostylus</i>					
CP9	<i>D. diastypus</i>	CP9b	<i>D. binodosus</i>	NP11		
		CP9a	<i>T. contortus</i>	NP10	└ <i>T. bramlettei</i>	
Paleocene	CP8	<i>D. multiradiatus</i>	CP8b	<i>C. eodela</i>	NP9	└ <i>D. multiradiatus</i>
			CP8a	<i>C. bidens</i>		
	CP7	<i>D. nobilis</i>			7/8	└ <i>H. riedelii</i>
	CP6	<i>D. mohleri</i>				└ <i>D. mohleri</i>
	CP5	<i>H. kleinpellii</i>			NP6	└ <i>H. kleinpellii</i>
	CP4	<i>F. tympaniformis</i>			NP5	└ <i>F. tympaniformis</i>
	CP3	<i>E. macellus</i>			NP4	└ <i>P. martinii/N. saepes</i>
	CP2	<i>C. danicus</i>			NP3	└ <i>C. danicus</i>
CP1	<i>Z. sigmoides</i>	CP1b	<i>C. tenuis</i>	NP2	└ <i>Cruciplacolithus (>7 μm)</i>	
		CP1a	<i>C. primus</i>	NP1	└ <i>B. sparsus</i>	

└ = First occurrence
┌ = last occurrence

Figure 3. Paleocene-Eocene coccolith biostratigraphic scheme of Okada and Bukry (1980) and number-coded scheme of Martini (1971). Datum levels used in this report are shown on the right.

Leg 113 USSAC Funds, an equipment grant from the Amoco Foundation, and a partial Aylesworth Foundation fellowship for the first author.

REFERENCES

Alvarez, W., Arthur, M. A., Fisher, A. G., Lowrie, W., Napoleone, G., Premoli-Silva, I., and Roggenthen, W. M., 1977. Upper Cretaceous-Paleocene magnetic stratigraphy at Gubbio, Italy. V. Type section for the Late Cretaceous-Paleogene geomagnetic reversal time scale. *Geol. Soc. Am. Bull.*, 88:367-389.

Angelozzi, G. N., 1988. Nanofosiles paleocenos del Noreste de la Cuenca Neuquina, Republica Argentina. *Ameghiniana*, 24:299-307.

Applegate, J. L., Wise, S. W., Jr., 1987. Eocene calcareous nannofossils, Deep Sea Drilling Project Site 605, upper continental rise off New Jersey, U.S.A. In van Hinte, J. E., Wise, S. W., Jr., et al. *Init. Repts. DSDP*, 93: Washington (U.S. Govt. Printing Office), 685-698.

Backman, J., 1986. Late Paleocene to middle Eocene calcareous nannofossil biochronology from the Shatsky Rise, Walvis Ridge and Italy. *Palaeogeogr., Palaeoclimatol., Palaeoecol.*, 57:43-59.

Barker, P. F., Dalziel, I.W.D., et al., 1977. *Init. Repts. DSDP*, 36: Washington (U.S. Govt. Printing Office).

Barker, P. F., Kennett, J. P., et al., 1988. *Proc. ODP, Init. Repts.*, 113: College Station, TX (Ocean Drilling Program).

Barr, F. T., and Berggren, W. A., 1981. Lower Tertiary biostratigraphy and tectonics of northeastern Libya. In Solem, M., and Buswiel,

- M.-T. (Eds.), *The Geology of Libya*: London (Academic Press), 1: 163-192.
- Berggren, W. A., Kent, D. V., and Flynn, J., 1985. Paleogene geochronology and chronostratigraphy. In Snelling, N. J. (Ed.), *The chronology of the geologic record*. Geol. Soc. London, 141-195.
- Bramlette, M. N., and Sullivan, F. R., 1961. Coccolithophorids and related nannoplankton of the Early Tertiary in California. *Micropaleontology*, 10:129-174.
- Bukry, D., 1973. Coccolith and silicoflagellate stratigraphy, Tasman Sea and Southeastern Pacific Ocean, Deep Sea Drilling Project Leg 21. In Burns, R. E., Andrews, J. E., et al., *Init. Repts. DSDP*, 21: Washington (U.S. Govt. Printing Office), 885-893.
- Edwards, A. R., 1973. Key species of New Zealand calcareous nannofossils. *N.Z. J. Geol. Geophys.*, 16:68-89.
- Haq, B. U., Hardenbol, J., and Vail, P. R., 1987. Chronology of fluctuating sea levels since the Triassic (250 million years ago to present): *Science*, 235:1156-1167.
- Hay, W. W., 1970. Calcareous Nannofossils from cores recovered on Leg 4. In Bader, R. G., Gerard, R. D., et al., *Init. Repts. DSDP*, 4: Washington (U.S. Govt. Printing Office), 455-502.
- Hay, W. W., and Towe, K. M., 1962. Electron microscope examination of some coccoliths from Donzacq (France). *Eclog. geol. Helv.*, 55: 497-515.
- Hay, W. W., and Mohler, H. P., 1967. Calcareous nannoplankton from early Tertiary rocks at Pont Labau, France, and Paleocene-Eocene correlations. *J. Paleontol.*, 41:1505-1541.
- Jiang, M. J., and Gartner, S., 1986. Calcareous nannofossil succession across the Cretaceous/Tertiary boundary in east-central Texas. *Micropaleontology*, 32:232-255.
- Loeblich, A. R., Jr., and Tappan, H., 1966. Annotated index and bibliography of the calcareous nannoplankton, I. *Phycologia*, 5:81-216.
- _____, 1968. Annotated index and bibliography of the calcareous nannoplankton, II. *J. Paleontol.*, 42:584-598.
- _____, 1969. Annotated index and bibliography of the calcareous nannoplankton, III. *J. Paleontol.*, 43:568-588.
- _____, 1970a. Annotated index and bibliography of the calcareous nannoplankton, IV. *J. Paleontol.*, 44:558-574.
- _____, 1970b. Annotated index and bibliography of the calcareous nannoplankton, V. *Phycologia*, 9:157-174.
- _____, 1971. Annotated index and bibliography of the calcareous nannoplankton, VI. *Phycologia*, 10:315-339.
- _____, 1973. Annotated index and bibliography of the calcareous nannoplankton, VII. *J. Paleontol.*, 47:715-759.
- Ludwig, W. J., Krasheninnikov, V. A., et al., 1983. *Init. Repts. DSDP*, 71: Washington (U.S. Govt. Printing Office).
- Martini, E., 1971. Standard Tertiary and Quaternary calcareous nannoplankton zonation. In Farinacci, A. (Ed.), *Proc. 2nd Plankt. Conf. Roma*: Rome (Edizioni Technoscienza), 2:739-85.
- Oberhänsli, H., MacKenzie, J. A., Toumarkine, M., and Weissert, T., 1984. A paleoclimatic and paleoceanographic record of the Paleogene in the Central South Atlantic (Leg 73, Sites 522, 523, and 524). In Hsü, K. J., LaBrecque, J. L., et al., *Init. Repts. DSDP*, 73: Washington (U.S. Govt. Printing Office), 737-747.
- Okada, H., and Bukry, D., 1980. Supplementary modification and introduction of code numbers to the low-latitude coccolith biostratigraphic zonation. *Mar. Micropaleontol.*, 5:321-325.
- Olsson, R. K., Gibson, T. G., Hansen, H. J., and Owens, J. P., 1988. Geology of the northern Atlantic coastal plain: Long Island to Virginia. In Sheridan, R. E., and Grow, J. A. (Eds.), *The Atlantic Continental Margin*: U.S., DNAG, 1-2:87-105.
- Perch-Nielsen, K., 1977. Albian to Pleistocene calcareous nannofossils from the Western South Atlantic, DSDP Leg 39, In Perch-Nielsen, K., Supko, P. R., et al., *Init. Repts. DSDP*, 39: Washington (U.S. Govt. Printing Office), 699-823.
- _____, 1979a. Calcareous nannofossil zonation at the Cretaceous/Tertiary boundary in Denmark. In Birkelund, T., and Bromley, R. G. (Eds.), *Cretaceous-Tertiary Boundary Events, Volume 1*: Copenhagen (Univ. Copenhagen), 115-135.
- _____, 1985. Mesozoic calcareous nannofossils. In Bolli, H. M., Saunders, J. B., and Perch-Nielsen, K. (Eds.), *Plankton Stratigraphy*: Cambridge, England (Cambridge Univ. Press), 329-426.
- Percival, S. F., Jr., 1984. Late Cretaceous to Pleistocene calcareous nannofossils from the South Atlantic, Deep Sea Drilling Project Leg 73. In Hsü, K. J., LaBrecque, J. L., et al., *Init. Repts. DSDP*, 73: Washington (U.S. Govt. Printing Office), 391-424.
- Poag, C. W., Reynolds, L. A., Mazzullo, J. M., and Keigwin, L. D., 1985. Foraminiferal, lithic, and isotopic changes across four major unconformities at Deep Sea Drilling Project Site 548, Goban Spur. In Graciansky, P. C. de, Poag, C. W., et al., *Init. Repts. DSDP*, 80: Washington (U.S. Govt. Printing Office), 539-555.
- Roth, P. H., 1973. Calcareous nannofossils—Leg 17, Deep Sea Drilling Project. In Winterer, E. L., Ewing, J. I., et al., *Init. Repts. DSDP*, 17: Washington (U.S. Govt. Printing Office), 695-795.
- Shackleton, N. J., and Kennett, J. P., 1975. Paleotemperature history of the Cenozoic and the initiation of Antarctic glaciation: Oxygen and carbon isotope analyses in DSDP Sites 277, 279, and 281. In Kennett, J. P., Houtz, R. E., et al., *Init. Repts. DSDP*, 29: Washington (U.S. Govt. Printing Office), 743-755.
- Shackleton, N. J., et al., 1984. Accumulation rates in Leg 74 sediments. In Moore, T. C., Jr., Rabinowitz, P. D., et al., *Init. Repts. DSDP*, 74: Washington (U.S. Govt. Printing Office), 621-644.
- Shackleton, N. J., Hall, M. A., and Boersma, A., 1984. Oxygen and carbon isotope data from Leg 74 foraminifers. In Moore, T. C., Jr., Rabinowitz, P. D., et al., *Init. Repts. DSDP*, 74: Washington (U.S. Govt. Printing Office), 599-611.
- Shipboard Scientific Party, 1988. Site Reports. In Barker, P. F., Kennett, J. P., et al., *Proc. ODP, Init. Repts.*, 113: College Station, TX (Ocean Drilling Program).
- Steinmetz, J. C., 1984a. Bibliography and taxa of calcareous nannoplankton, III. *Int. Nannoplankton Assoc. Newsl.*, 6:6-37.
- _____, 1984b. Bibliography and taxa of calcareous nannoplankton, IV. *Int. Nannoplankton Assoc. Newsl.*, 6:55-81.
- _____, 1985a. Bibliography and taxa of calcareous nannoplankton, V. *Int. Nannoplankton Assoc. Newsl.*, 7:5-28.
- _____, 1985b. Bibliography and taxa of calcareous nannoplankton, IV. *Int. Nannoplankton Assoc. Newsl.*, 7:122-144.
- _____, 1986. Bibliography and taxa of calcareous nannoplankton, VIII. *Int. Nannoplankton Assoc. Newsl.*, 8:66-82.
- _____, 1987a. Bibliography and taxa of calcareous nannoplankton, IX. *Int. Nannoplankton Assoc. Newsl.*, 9:8-26.
- _____, 1987b. Bibliography and taxa of calcareous nannoplankton, X. *Int. Nannoplankton Assoc. Newsl.*, 9:79-105.
- _____, 1988a. Bibliography and taxa of calcareous nannoplankton, XI. *Int. Nannoplankton Assoc. Newsl.*, 10:7-28.
- _____, 1988b. Bibliography and taxa of calcareous nannoplankton, XII. *Int. Nannoplankton Assoc. Newsl.*, 10:60-80.
- _____, 1989. Bibliography and taxa of calcareous nannoplankton, XIII. *Int. Nannoplankton Assoc. Newsl.*, 11:6-20.
- Thierstein, H. R., 1982. Terminal Cretaceous plankton extinctions: a critical assessment. *Spec. Pap. Geol. Soc. Am.*, 190:385-399.
- Vail, P. R., Mitchum, R. M., Todd, R. G., Widmier, J. M., Thompson III, S., Sangree, J. B., Bubba, J. N., and Hatelid, W. G., 1977. Seismic stratigraphy and global changes of sea level. In Payton, C. E. (Ed.), *Seismic Stratigraphy—Applications to Hydrocarbon Exploration*, Am. Assoc. Petrol. Geol. Mem., 26:49-205.
- Varol, O., 1989. Paleocene calcareous nannofossil biostratigraphy. In Crux, J. A., and Heck, S. E. van (Eds.), *Nannofossils and Their Applications*: New York (Wiley), 267-310.
- Wei, W., and Wise, S. W., Jr., 1989. Paleogene calcareous nannofossil magnetobiochronology: Results from South Atlantic DSDP Site 516. *Mar. Micropaleontol.*, 14:119-152.
- Wind, F. H., and Wise, S. W., Jr., 1977. Systematic paleontology. In Wise, S. W., Jr., and Wind, F. H., Mesozoic and Cenozoic calcareous nannofossils recovered by DSDP Leg 36 drilling on the Falkland Plateau, Southwest Atlantic sector of the Southern Ocean. In Barker, P. F., Dalziel, I.W.D., et al., *Init. Repts. DSDP*, 36: Washington (U.S. Govt. Printing Office), 295-309.
- _____, 1983. Correlation of upper Campanian-lower Maestrichtian calcareous nannofossil assemblages in drill and piston cores from the Falkland Plateau, southwest Atlantic Ocean. In Ludwig, W. J., Krasheninnikov, V. A., et al., *Init. Repts. DSDP*, 71: Washington (U.S. Govt. Printing Office), 551-563.
- Wise, S. W., Jr., 1983. Mesozoic and Cenozoic calcareous nannofossils recovered by Deep Sea Drilling Project Leg 71 in the Falkland Plateau region, southwest Atlantic Ocean. In Ludwig, W. J., Krasheninnikov, V. A., et al., *Init. Repts. DSDP*, Leg 71: Washington (U.S. Govt. Printing Office), 481-550.
- Wise, S. W., Jr., and Wind, F. H., 1977. Mesozoic and Cenozoic calcareous nannofossils recovered by DSDP Leg 36 drilling on the Falkland Plateau, Southwest Atlantic sector of the Southern Ocean. In

Barker, P. F., Dalziel, I.W.D., et al., *Init. Repts. DSDP*, 36: Washington (U.S. Govt. Printing Office), 269-491.

Date of initial receipt: 27 February 1989
Date of acceptance: 19 September 1989
Ms 113B-205

APPENDIX

Cenozoic Calcareous Nannofossils Considered in this Report (In alphabetical order of generic epithets)

- Amithalithina sigmundii* n. gen., n. sp.
Biantholithus sparsus Bramlette and Martini, 1964
Biscutum castrorum Black, 1959
B. neocoronum n. sp.
Biscutum sp.
Chiasmolithus bidens (Bramlette and Sullivan) Hay and Mohler, 1967
C. consuetus (Bramlette and Sullivan) Hay and Mohler, 1967
C. danicus (Brotzen) Hay and Mohler, 1967
C. eograndis Perch-Nielsen, 1971d
C. expansus (Bramlette and Sullivan) Gartner, 1970
C. grandis (Bramlette and Riedel) Radomski, 1968
C. solitus (Bramlette and Sullivan) Locker, 1968
Chiasmolithus sp.
Coccolithus cavus (Hay and Mohler) Perch-Nielsen, 1969
C. formosus (Kamptner) Wise, 1973
C. pelagicus (Wallich) Schiller, 1930
C. sp. cf. *C. pelagicus*
Cruciplacolithus asymmetricus van Heck and Prins, 1987
C. edwardsii Romein, 1979
C. intermedius van Heck and Prins, 1987
C. primus Perch-Nielsen, 1977
C. tenuis (Stradner) Hay and Mohler, 1967
Cyclagelosphaera reinhardtii (Perch-Nielsen) Romein, 1977
Cyclicargolithus sp. cf. *C. luminis*
Discoaster barbadiensis Tan, 1927
D. bifax Bukry, 1971a
D. sp. cf. *D. bifax*
D. binodosus Martini, 1958
D. sp. cf. *D. binodosus*
D. deflandrei Bramlette and Riedel, 1954
D. sp. cf. *D. deflandrei*
D. diastypus Bramlette and Sullivan, 1961
D. sp. cf. *D. diastypus*
D. elegans Bramlette and Sullivan, 1961
D. falcatus Bramlette and Sullivan, 1961
D. kuepperi Stradner, 1959a
D. sp. cf. *D. kuepperi*
D. lenticularis Bramlette and Sullivan, 1961
D. lodoensis Bramlette and Riedel, 1954
D. mediosus Bramlette and Sullivan, 1961
D. megastypus Bramlette and Sullivan, 1961
D. mohleri Bukry and Percival, 1971
D. multiradiatus Bramlette and Riedel, 1954
D. nobilis Martini, 1961a
D. sp. cf. *D. nobilis*
D. sublodoensis Bramlette and Sullivan, 1961
Discoaster sp.
Ellipsolithus distichus (Bramlette and Sullivan) Sullivan, 1964
E. lajollaensis Bukry and Percival, 1971
Ericsonia subpertusa Hay and Mohler, 1967
Fasciculithus involutus Bramlette and Sullivan, 1961
F. tympaniformis Hay and Mohler, 1967
F. sp. cf. *F. tympaniformis*
Heliolithus cantabriae Perch-Nielsen, 1971d
H. kleinpellii Sullivan, 1964
H. riedelii Bramlette and Sullivan, 1961
H. sp. cf. *H. riedelii*
H. universus Wind and Wise, 1977
H. sp. cf. *H. universus*
Heliolithus sp.
Hornibrookina australis Edwards and Perch-Nielsen, 1975
H. edwardsii Perch-Nielsen, 1977
H. teuriensis Edwards, 1973a
Lapideacassis sp.
Markalius apertus Perch-Nielsen, 1979a
M. inversus (Deflandre) Bramlette and Martini, 1964
Nannotetrina cristata (Martini) Perch-Nielsen, 1971d
N. fulgens (Stradner) Achutan and Stradner, 1969
Neochiastozygus cearae Perch-Nielsen, 1977
N. distentus (Bramlette and Sullivan) Perch-Nielsen, 1971c
N. eosaepes Perch-Nielsen, 1981a
N. junctus (Bramlette and Sullivan) Perch-Nielsen, 1971c
N. sp. cf. *N. modestus* Perch-Nielsen, 1971c
N. perfectus Perch-Nielsen, 1971c
N. saepes Perch-Nielsen, 1971c
Neochiastozygus sp.
Neococcolithes dubius (Deflandre) Black, 1967
N. protenus (Bramlette and Sullivan) Black, 1967
N. sp. cf. *N. protenus*
Neocrepidolithus cruciatus (Perch-Nielsen) Perch-Nielsen, 1981a
Neocrepidolithus sp.
Pontosphaera sp.
Prinsius bisulcus (Stradner) Hay and Mohler, 1967
P. dimorphosus (Perch-Nielsen) Perch-Nielsen, 1977
P. martinii (Perch-Nielsen) Haq, 1971
P. sp. cf. *P. tenuiculum* (Okada and Thierstein) Perch-Nielsen, 1984a
Reticulofenestra daviesii (Haq) Haq, 1971
R. onustus (Perch-Nielsen) Wise, 1983
R. reticulata (Gartner) Roth, 1973
R. samodurovii (Hay, Mohler, and Wade) Bukry and Percival, 1971
Reticulofenestra sp.
Sphenolithus editus Perch-Nielsen, 1978
S. moriformis (Brönnimann and Stradner) Bramlette and Wilcoxon, 1967
S. radians Deflandre, 1952
Thoracosphaera crassa van Heck and Prins, 1987
T. operculata Bramlette and Martini, 1964
Thoracosphaera sp.
Toweius callosus Perch-Nielsen, 1971d
T. craticulus Hay and Mohler, 1967
T.? *crassus* (Bramlette and Sullivan) Perch-Nielsen, 1984a
T. eminens (Bramlette and Sullivan) Perch-Nielsen, 1971b
T.? *magnicrassus* (Bukry) Romein, 1979
T. selandius Perch-Nielsen, 1979a
T. tovae Perch-Nielsen, 1971b
T. sp. cf. *T. tovae*
Tribrachiatum bramlettei (Brönnimann and Stradner) Proto Decima et al., 1975
T. contortus (Stradner) Bukry, 1972
T. orthostylus Shamrai, 1963
Zygodiscus herlynii Sullivan, 1964
Z. sigmoides Bramlette and Sullivan, 1961
Zygrhablithus bijugatus (Deflandre) Deflandre, 1959

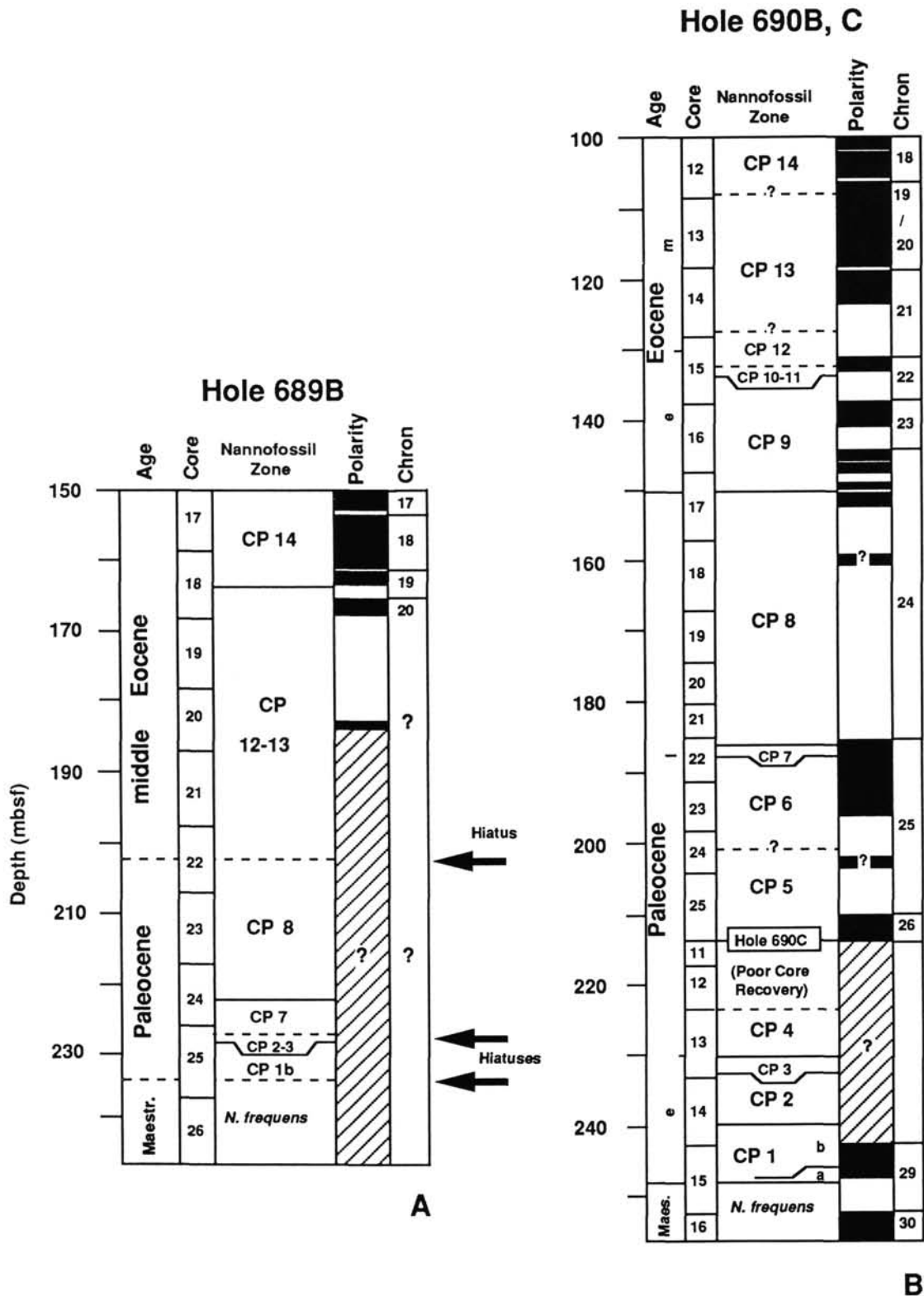


Figure 4. Summary of calcareous nannofossil biostratigraphy correlated with magnetostratigraphy of Hamilton (this volume) (Cretaceous-lowermost Paleocene) and Spieß (written comm., 1989). **A.** Hole 689B. **B.** Holes 690B and 690C. Hiatuses are indicated by arrows for Hole 689B. black = normal polarity, white = reversed polarity, striped = polarity uncertain.

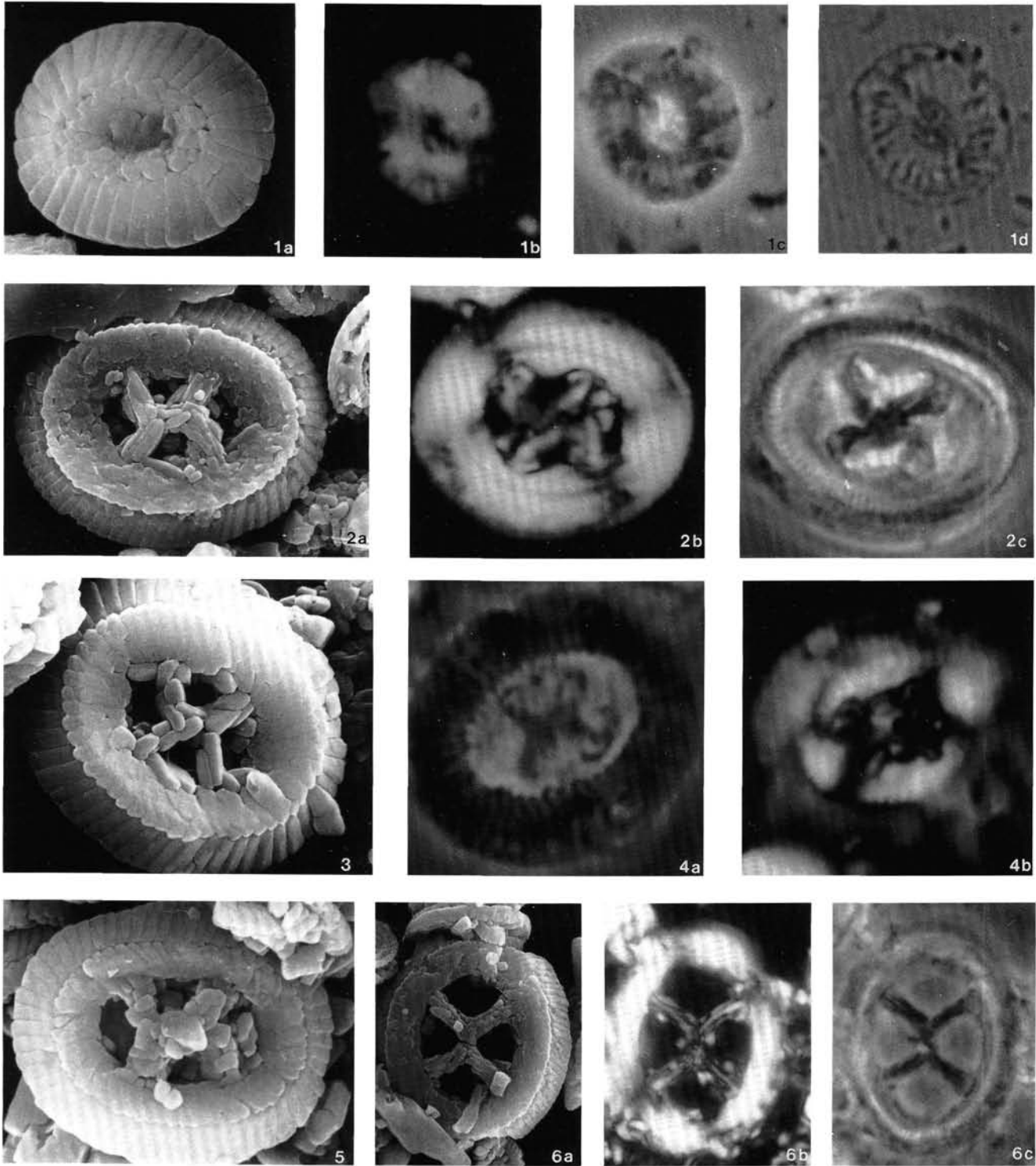


Plate 1. Note on the plates: All micrographs of coccoliths are of the distal view except where noted otherwise. Pol, Ph, Tr, and SEM denote polarized, phase contrast, transmitted, and scanning electron micrographs respectively. Where more than one illustration is provided of a specimen, the sample and magnification designation are not repeated in the caption. **1.** *Biscutum? neocoronum* n. sp., Sample 113-690B-17H-7, 28-30 cm (a) SEM, Holotype, $\times 6300$; (b-d) Isotype, $\times 3500$; (b) Pol; (c) Ph; (d) Tr. **2.** *Chiasmolithus bidens*, Section 113-690B-19H, CC (a) SEM, $\times 4400$; (b) Pol, $\times 3300$; (c) Ph. **3.** *Chiasmolithus* sp. cf. *C. consuetus*, Sample 113-690C-13X-1, 28-30 cm, SEM, $\times 6900$. **4.** *Chiasmolithus consuetus*, Sample 113-690B-16H-6, 28-30 cm (a) Ph, $\times 3750$; (b) Pol. **5.** *Chiasmolithus danicus*, Sample 113-690C-14X-3, 28-30 cm, SEM, $\times 6400$. **6.** *Chiasmolithus expansus*, Sample 113-690B-15H-4, 30-32 cm (a) SEM, $\times 2750$; (b) Pol, $\times 2000$; (c) Ph.

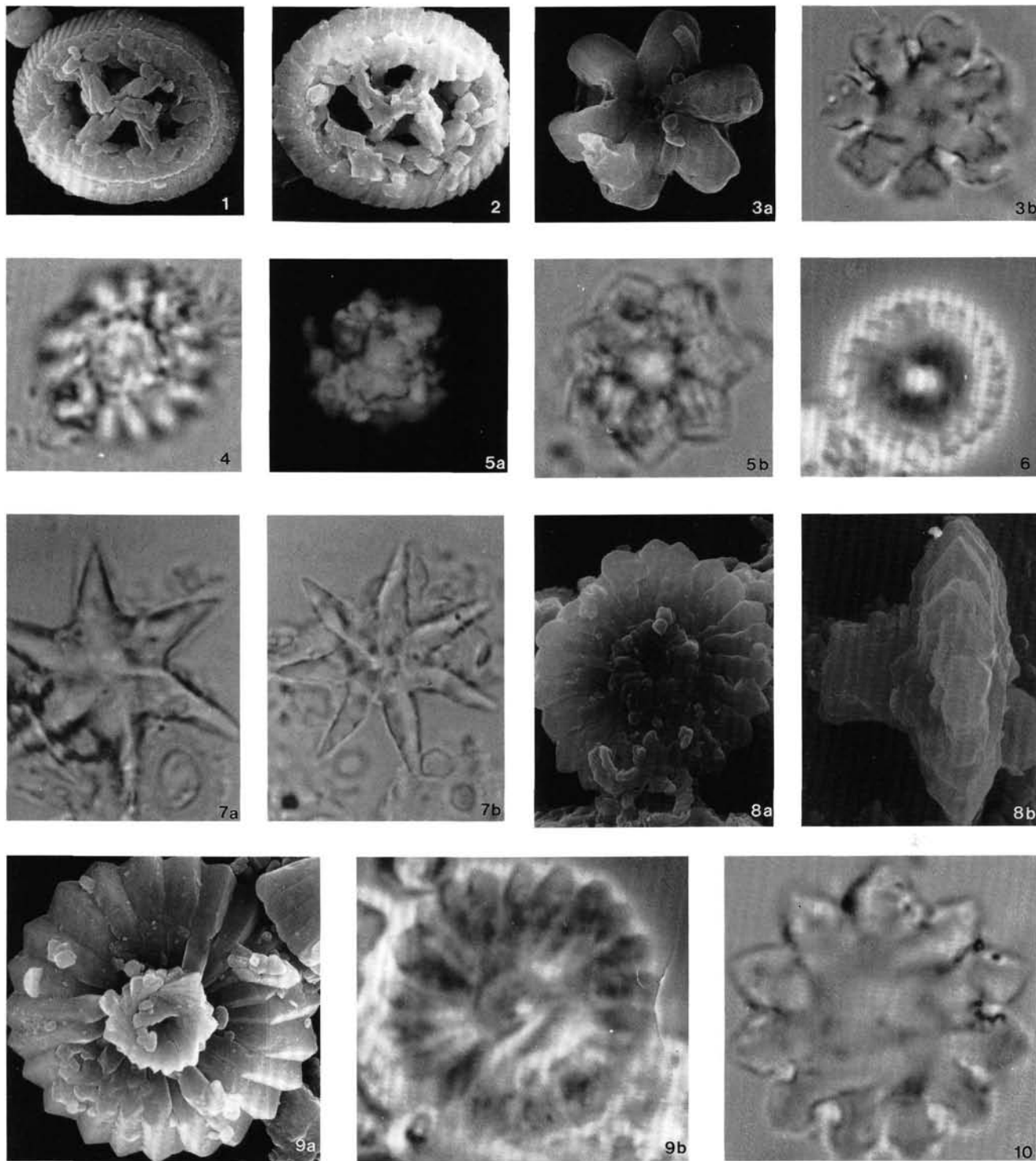


Plate 2. 1. *Chiasmolithus solitus*, Sample 113-690B-16H-5, 28-30 cm, SEM, $\times 3100$. 2. *Chiasmolithus* sp., Sample 113-690B-16H-5, 28-30 cm, SEM, $\times 6300$. 3. *Discoaster* sp. cf. *D. deflandrei*, (a) Sample 113-690B-15H-4, 30-32 cm, SEM, $\times 4700$; (b) Sample 113-690B-15H-2, 30-32 cm, Tr, $\times 4400$. 4. *Discoaster kuepperi*, Sample 113-690B-17H-1, 28-30 cm, Tr, $\times 3400$. 5. *Discoaster* sp. cf. *D. kuepperi* Sample 113-690B-15H-5, 30-32 cm (a) Pol, $\times 2800$; (b) Tr, $\times 3100$. 6. *Discoaster lenticularis*, Section 113-690B-19H, CC, Ph, $\times 3000$. 7. *Discoaster lodoensis*, Sample 113-690B-15H-3, 30-32 cm (a) Tr, $\times 3100$; (b) Tr, different specimen, $\times 3100$. 8. *Discoaster* sp. cf. *D. megastypus*, Sample 113-690B-19H-3, 29-31 cm (a) SEM, $\times 4100$; (b) SEM, $\times 5400$. 9. *Discoaster multiradiatus*, Section 113-690B-19H, CC (a) SEM, $\times 5400$; (b) Ph, $\times 3200$. 10. *Discoaster* sp. cf. *D. binodosus*, Sample 113-690B-17H-1, 28-30 cm, Tr, $\times 3100$.

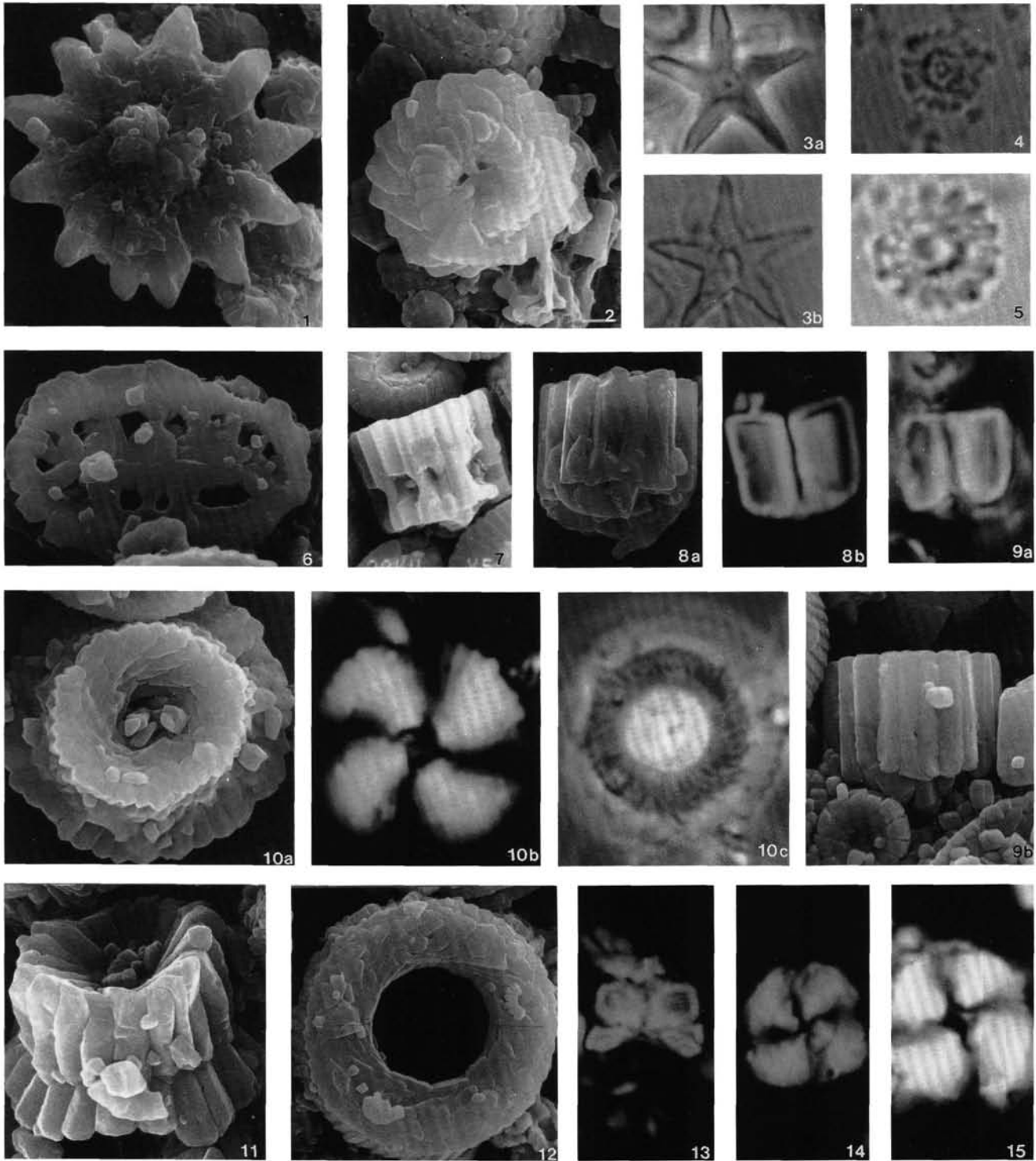


Plate 3. 1. *Discoaster* sp. cf. *D. nobilis*, Sample 113-690B-19H-3, 29–31 cm, SEM, $\times 2500$. 2. *Discoaster* sp., Sample 113-690B-19H-3, 29–31 cm, SEM, $\times 5600$. 3. *Discoaster sublodoensis*, Sample 113-690B-15H-3, 30–32 cm (a) Ph, $\times 2900$; (b) Tr. 4. *Discoaster* sp. cf. *D. bifax*, Sample 113-690B-15H-1, 30–32 cm, Tr, $\times 2300$. 5. *Discoaster* sp. cf. *D. bifax*, Section 113-690B-16H, CC, Ph, $\times 2900$. 6. *Ellipsolithus distichus*, Sample 113-690B-22H-2, 28–30 cm, SEM, $\times 5900$. 7. *Fasciculithus involutus*, Sample 113-690B-22H-4, 28–30 cm, SEM, $\times 3500$. 8. *Fasciculithus tympaniformis* (a) Sample 113-690B-15H-4, 30–32 cm, SEM, $\times 4300$; (b) Section 113-690B-19H, CC, Pol, $\times 3300$. 9. *Fasciculithus* sp. cf. *F. tympaniformis* (a) Sample 113-690C-13X-3, 129–131 cm, Pol, $\times 3950$; (b) Section 113-690C-13X, CC, SEM, $\times 5600$. 10. *Heliolithus kleinpellii*, Section 113-690B-25H, CC (a) SEM, $\times 5500$; (b) Pol, $\times 3250$; (c) Ph. 11. *Heliolithus riedelii*, Section 113-689B-24X, CC, SEM, $\times 5600$. 12. *Heliolithus* sp. cf. *H. universus*, Sample 113-690B-22H-2, 28–30 cm, SEM, $\times 4350$. 13. *Heliolithus* sp. cf. *H. riedelii*, Sample 113-690B-22H-2, 28–30 cm, Pol, $\times 2500$. 14. *Heliolithus* sp., Sample 113-690B-22H-2, 28–30 cm, Pol, $\times 2350$. 15. *Heliolithus cantabriae*, Section 113-690B-25H, CC, Pol, $\times 1900$.

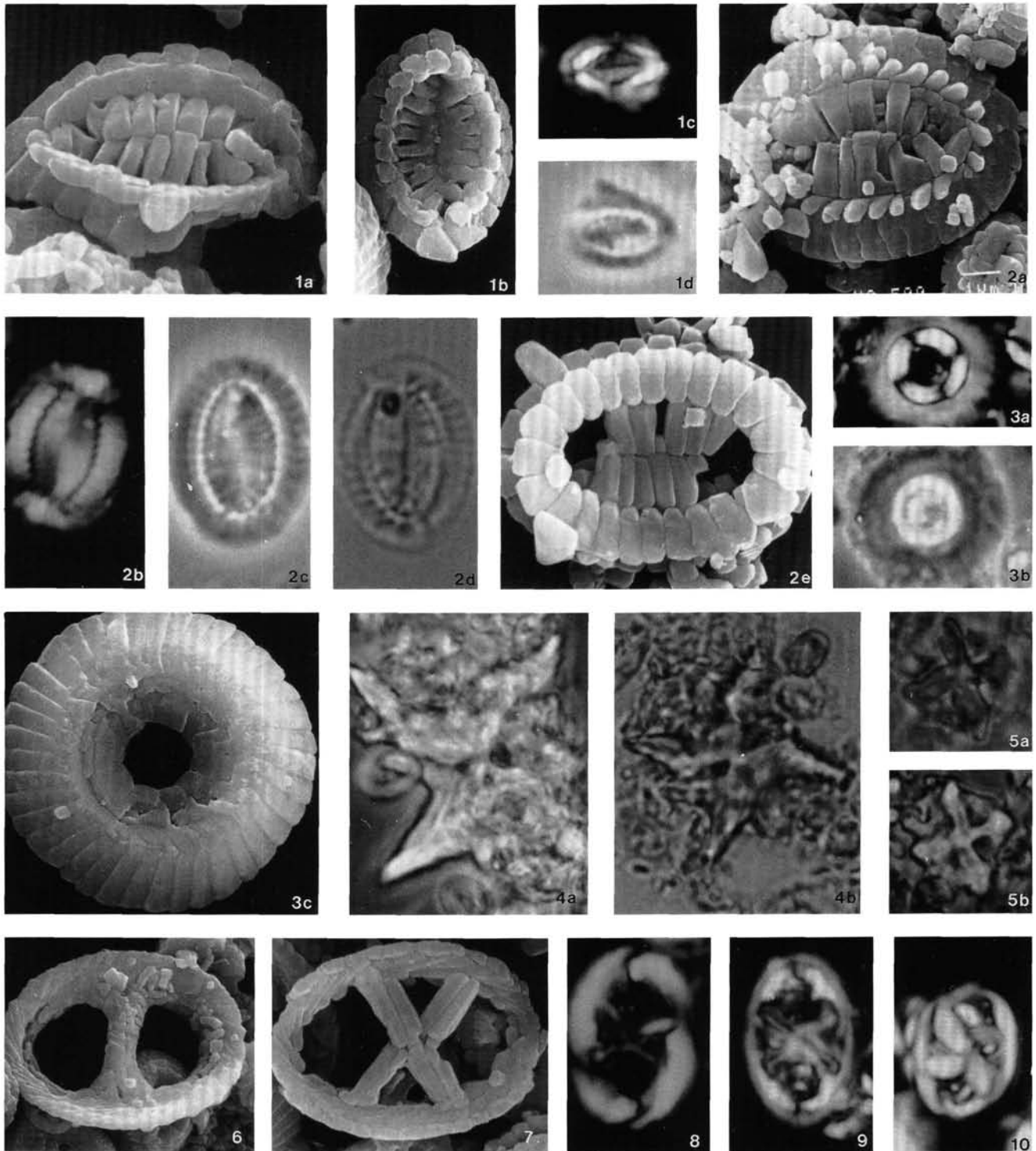


Plate 4. 1. *Hornibrookina australis* (a) Sample 113-690B-22H-2, 28-30 cm, SEM, $\times 9600$ (b) Sample 113-690B-16H-5, 28-30 cm, SEM, $\times 7200$, proximal view; (c) Sample 113-690B-16H-6, 28-30 cm, Pol, $\times 3750$; (d) Ph. 2. *Hornibrookina teuriensis*, Sample 113-690C-13X-5, 129-131 cm (a) SEM, $\times 6000$; (b) Pol, $\times 3100$; (c) Ph; (d) Tr; (e) SEM, $\times 8000$, proximal view. 3. *Markalius apertus* (a) Section 113-690B-15H, CC, Pol, $\times 2400$; (b) Ph; (c) Section 113-690B-25H, CC, SEM, $\times 5800$. 4. *Nannotetrina fulgens*, Sample 113-689B-19H-1, 30-32 cm (a) Ph, $\times 1700$; (b) Tr, $\times 1800$, different specimen. 5. *Nannotetrina cristata*, Sample 113-689B-19H-1, 30-32 cm (a) Tr, $\times 1500$; (b) Ph. 6. *Neochiastozygus cearae*, Section 113-690B-23H, CC, SEM, $\times 2600$. 7. *Neochiastozygus* sp. cf. *N. modestus*, Sample 113-690B-22H-2, 28-30 cm, SEM, $\times 6000$. 8. *Neochiastozygus distentus*, Sample 113-690B-16H-1, 28-30 cm, Pol, $\times 3100$. 9. *Neochiastozygus saepes*, Sample 113-690C-13X-5, 129-131 cm, Pol, $\times 3000$. 10. *Neococcolithes* sp. cf. *N. protenus*, Section 113-690B-19H, CC, Pol, $\times 3200$.

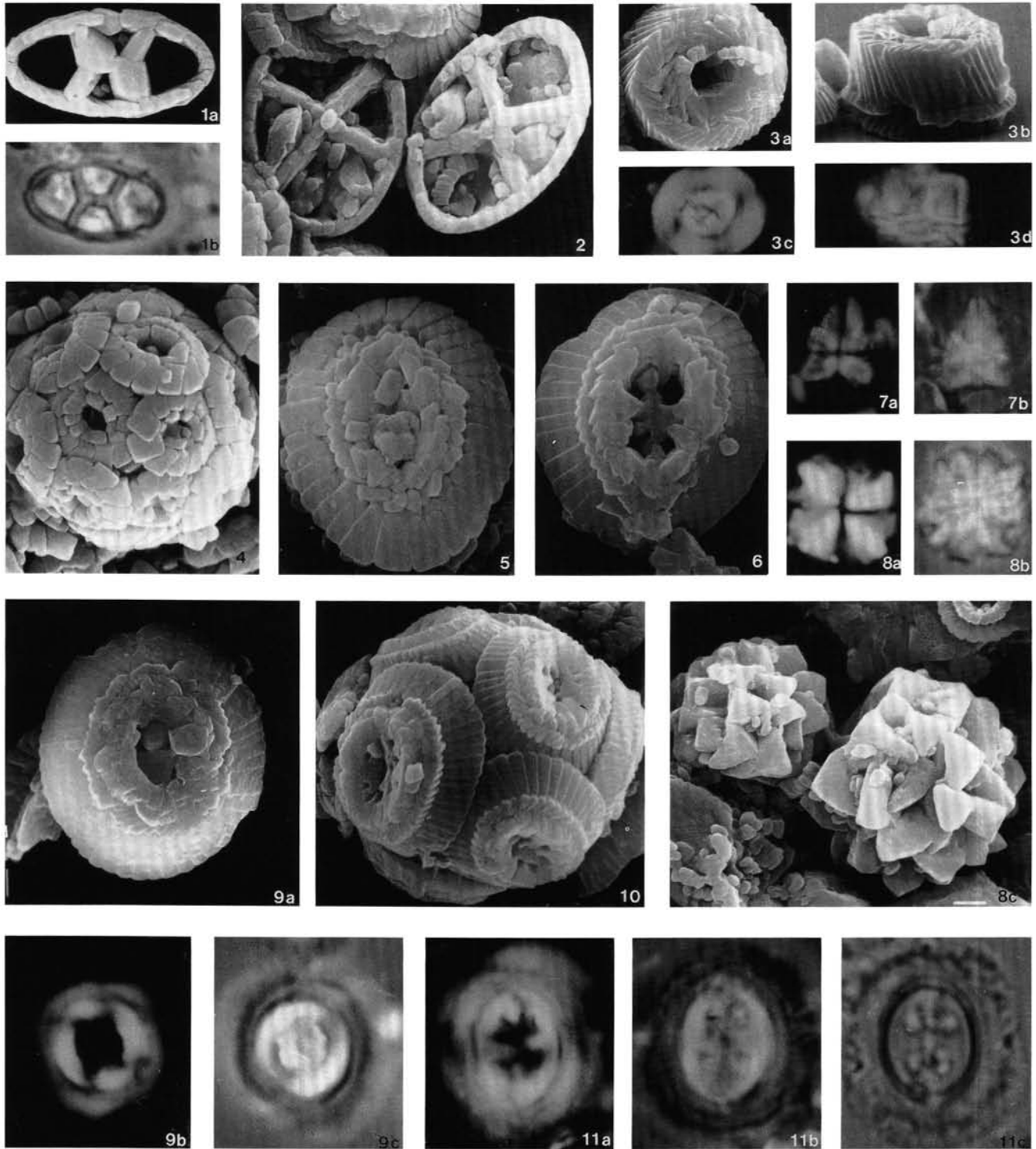


Plate 5. 1. *Neococcolithes dubius* (a) Sample 113-690B-15H-4, 30-32 cm, SEM, $\times 4500$; (b) Sample 113-690B-22H-4, 28-30 cm, Ph, $\times 2700$. 2. *Neococcolithes protenus*, Sample 113-690B-22H-4, 28-30 cm, SEM, $\times 6200$. 3. *Amithalithina sigmundii*, n. gen., n. sp., (a) Sample 113-690B-15H-1, 30-32 cm, SEM, $\times 4500$; (b) SEM, $\times 4500$, side view of specimen (a); (c) Sample 113-690B-15H-3, 30-32 cm, Pol, $\times 3300$; (d) Pol, $\times 3300$, side view. 4. *Prinsius dimorphosus*, Sample 113-690C-14X-3, 28-30 cm, SEM, $\times 6400$, coccosphere. 5. *Prinsius martinii*, Sample 113-690B-22H-4, 28-31 cm, SEM, $\times 9600$. 6. *Prinsius bisulcus*, Sample 113-690B-22H-2, 28-30 cm, SEM, $\times 6900$. 7. *Sphenolithus editus*, Sample 113-690B-15H-5, 30-32 cm (a) Pol, $\times 2500$; (b) Ph. 8. *Sphenolithus moriformis*, Section 113-690B-19H, CC (a) Pol, $\times 4650$; (b) Ph; (c) SEM, $\times 4900$. 9. *Toweius callosus*, (a) Sample 113-690B-17H-7, 28-30 cm, SEM, $\times 4700$; (b) Section 113-690B-19H, CC, Pol, $\times 3300$; (c) Ph. 10. *Toweius craticulus*, Sample 113-690B-22H-4, 28-30 cm, SEM, $\times 4400$, coccosphere. 11. *Toweius emineus*, Section 113-690B-19H, CC; (a) Pol, $\times 3300$; (b) Ph; (c) Tr.

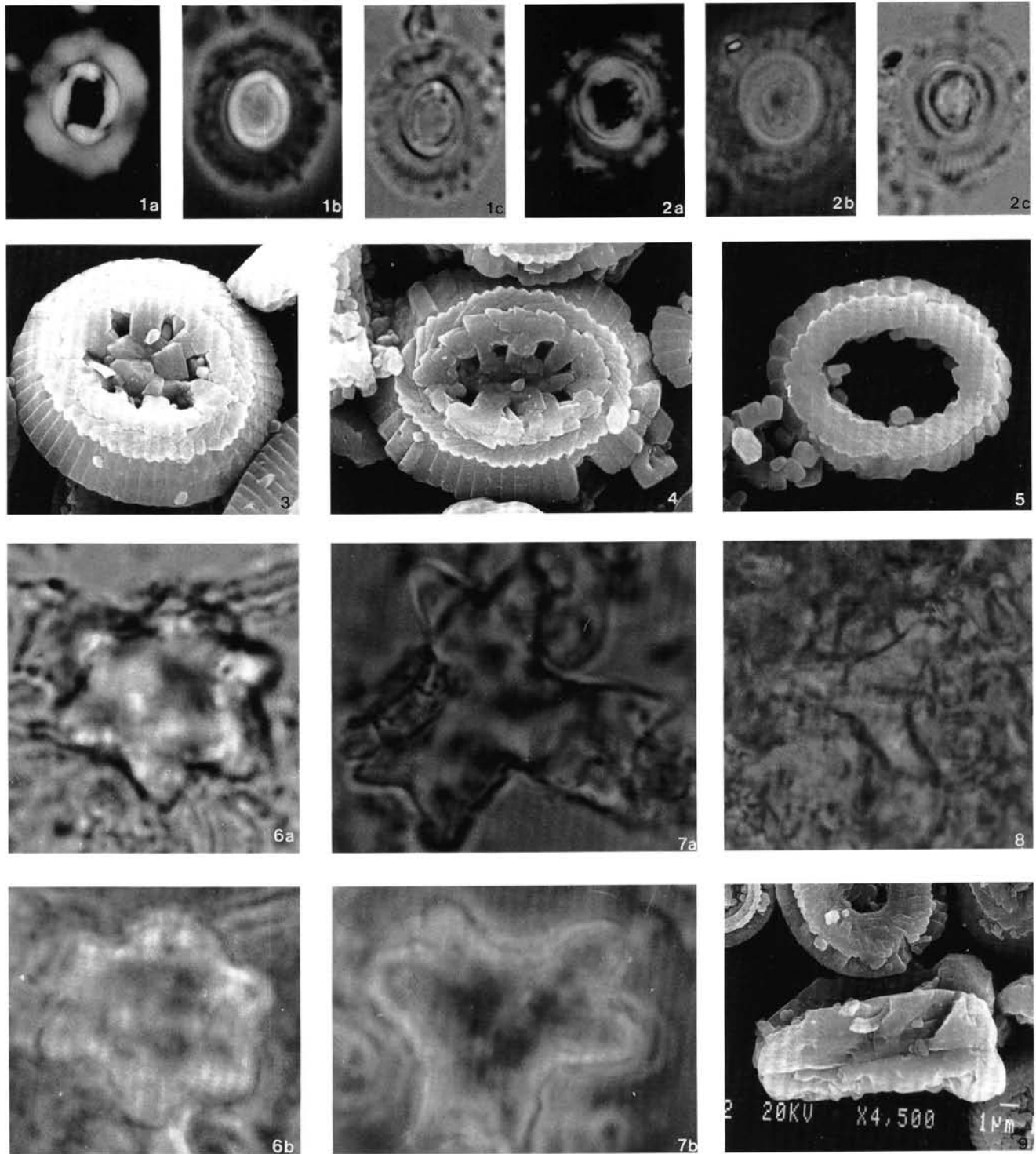


Plate 6. 1. *Toweius? crassus*, Section 113-690B-15H, CC (a) Pol, $\times 2700$; (b) Ph; (c) Tr. 2. *Toweius? magnicrassus*, Sample 113-690B-15H-2, 30-32 cm (a) Pol, $\times 2200$; (b) Ph; (c) Tr. 3. *Toweius tovae*, Section 113-690B-19H, CC, SEM, $\times 4800$. 4. *Toweius* sp. cf. *T. tovae*, Section 113-690B-19H, CC, SEM, $\times 5000$. 5. *Toweius selandius*, Sample 113-690C-13X-6, 28-30 cm, SEM, $\times 7300$. 6. *Tibrachiatus bramlettei*, Sample 113-690B-17H-1, 28-30 cm (a) Tr, $\times 3300$; (b) Ph. 7. *Tibrachiatus contortus*, (a) Sample 113-690B-16H-1, 28-30 cm, Tr, $\times 3000$; (b) Sample 113-690B-16H-1, 28-30 cm, Ph, $\times 3000$, different specimen. 8. *Tibrachiatus orthostylus*, Sample 113-690B-15H-2, 30-32 cm, Tr, $\times 1900$. 9. *Zygrhablithus bijugatus*, Section 113-690B-19H, CC, SEM, $\times 2900$.